

# **International Journal of Research in Pharmaceutical Sciences (IJRPS)**

**Volume No. 15**

**Issue No. 1**

**January - April 2024**



**ENRICHED PUBLICATIONS PVT. LTD**

**S-9, IInd FLOOR, MLU POCKET,  
MANISH ABHINAV PLAZA-II, ABOVE FEDERAL BANK,  
PLOT NO-5, SECTOR-5, DWARKA, NEW DELHI, INDIA-110075,  
PHONE: - + (91)-(11)-47026006**

# International Journal of Research in Pharmaceutical Sciences (IJRPS)

## **Aims and Scope**

International Journal of Research in Pharmaceutical Sciences (IJRPS) is publishing online peer reviewed scientific journal sponsored by JK Welfare & Pharmascope Foundation. The journal publishes research articles, review articles, short communications, case studies and reports in Pharmaceutical Sciences.

International Journal of Research in Pharmaceutical Sciences (IJRPS) is quarterly publishing online peer-reviewed scientific journal sponsored by JK Welfare & Pharmascope Foundation. The journal publishes research articles, review articles, short communications, case studies and reports in Pharmaceutical Sciences.

**Coverage Area:** Pharmaceutics, Novel Drug Delivery Systems, Pharmaceutical Chemistry and Drug Design, Pharmaceutical Analysis and Quality Assurance, Pharmaceutical Nanotechnology, Pharmacology and Toxicology, Hospital and Clinical Pharmacy, Clinical Research, Clinical Report, Case Studies, Pharmacognosy and Phytochemistry, Chemistry, Medical Biochemistry, Natural Products, Medicinal Chemistry, Molecular Biology, Microbiology and Biotechnology, Alternative Medicine, Polymer Science, Industrial Pharmacy, Drug Regulatory Affair, Intellectual Property Rights (IPR), Molecular Modeling, Herbal Medicines, Dental Medicines, Paramedical and Lifesciences.

# International Journal of Research in Pharmaceutical Sciences (IJRPS)

## EDITOR-IN-CHIEF

· **Dr. K. Gnanaprakash,**

Saastra College of Pharmaceutical Education & Research,  
Jawaharlal Nehru Technological University, Anantapur, India

## EDITORS

**D. Dachinamoorthy,**

Jawaharlal Nehru Technological University, Kakinada, India

## ASSOCIATE EDITORS

**K. B. Chandra Sekhar,**

Dept. of Chemistry, Jawaharlal Nehru Technological  
University, Anantapuramu-515 001, India

**N. Devanna,**

Dept. of Chemistry, Jawaharlal Nehru Technological  
University, Anantapuramu-515 001, India

**Omathanu Perumal,**

South Dakota State University, USA

**Sham S. Kakar,**

University of Louisville, USA

**Narasimman Gurusamy,**

Dept. of Anesthesiology and Medicine, Brigham and  
Womens Hospital, USA

**Ibrahim Darwish,**

King Saud University, Saudi Arabia

**CN. Ramchand,**

President and CEO, Laila Pharmaceuticals Pvt. Ltd.,  
Chennai, India

**J. Ashok Kumar,**

Department of Pharmaceutical Technology, Faculty of  
Pharmaceutical Sciences, UCSI University, Kuala  
Lumpur, Malaysia

**Lakshmi T,**

Associate Professor, Department of Pharmacology,  
Saveetha Dental College and Hospitals, Chennai, India

## EDITORIAL BOARD MEMBERS

**Prof. Dr. V. Gopal,**

Registrar Academic, Principal, Mother Theresa Post  
graduate and Research Institute of Health Sciences, (A  
Govt. of Puducherry Institution) Puducherry-6, India

**Riccardo Leardi,**

Italy

**Carmen Sanmartín,**

Universidad De Navarra, Spain

**Dr. C. Madhusudhana Chetty,**

Jawaharlal Nehru Technological University, Anantapur,  
India

**S. Uma Devi,**

Rajiv Gandhi University of Health and Sciences,  
Bengaluru, India

**K. G. Revikumar,**

Amrita Institute of Medical Sciences & Research Centre,  
Cochin, India

**Jintamai Suwanprateeb,**

National Metal and Materials Technology Center,  
Thailand

**Emmanuel udo etuk,**

Usmanu Danfodiyo University, Sokoto, Nigeria

**M. A. Ayub Shah,**

Dept. of Pharmacology & Toxicology, Central  
Agricultural University, Aizawl, Mizoram, India

**K. Lakshman,**

Dept. of Pharmacognosy, PES College of Pharmacy,  
Hanumanthnagar, Bangalore, India

|   |   |
|---|---|
| <b>Jayant Khandare,</b><br>Senior Research Scientist, Polymer Chem Grp, Piramal<br>Life Sciences Ltd., Mumbai, India  | <b>Shivanand P. Puthli,</b><br>Panacea Biotec Ltd., Mumbai, India   |
| <b>Sunil Agnihotri,</b><br>Frontage Laboratories Inc, USA   | <b>R. Praveen,</b><br>Bangalore, India  |
| <b>B. C. Behera,</b><br>Scientist, Agharkar Research Institute, Pune, India   | <b>Prakash. MMS. Kinthada,</b><br>Department of Chemistry, GIT, GITAM University,<br>Visakhapatnam, India |
| <b>P. Srinivasa Babu,</b><br>Principal, Vignan Pharmacy College, Vadlamudi, Andhra<br>Pradesh, India  | <b>Abbas S. Dakhil,</b><br>Assistant Professor, College of Medicine, University of<br>Al-Qadisiyah, Iraq  |
| <b>Dr. Anjaneyulu V,</b><br>Sr. Research Scientist in Manufacturing Science &<br>Technology, Technical Operations at Alembic<br>Pharmaceuticals Ltd, Vadodara, Gujarat, India | <b>Dr. Maytham T. Qasim,</b><br>College of Health and Medical Technology, Al-Ayen<br>University, Iraq     |
| <b>Dr. Zahraa Mohammed Ali Hamodat,</b><br>College of Science, University of Mosul, Iraq  | <b>Dr. Ahmed Ali Obaid,</b><br>College of Medicine, University of Al-Qadisiyah, Iraq                      |
| <b>Dr. Anwar Saleh Saihood Alkinani,</b><br>College of Medicine, University of Al-Qadisiyah, Iraq   |   |

# International Journal of Research in Pharmaceutical Sciences (IJRPS)

(Volume No. 15, Issue No.1, January - April 2024)

## Contents

| Sr. No. | Articles / Authors Name   | Pg. No. |
|---------|---|---------|
| 1       | Development and Validation of a simple UV spectrophotometric method for the determination of Delamanid<br><i>- Vaishali Pardeshi, Tushar Lokhande, Rina Firke, Sneha Patil, Vishakha Pawar</i>  | 01 - 08 |
| 2       | Diagnostic Aids and Techniques of Oral Cancer- An Updated Review<br><i>- Deivanayagi M1, Afreen Fathima I2</i>  | 09 - 18 |
| 3       | Etiological Evaluation of Microcytic Hypochromic Anemia at a Tertiary Care Hospital in the Eastern Part of India<br><i>-Prabhat Kumar1, Arun Kumar Singh1, Anju Bharti2, Sandeep Kumar1, Chanda Hemaliya3, Sandip Kumar2, Lalit Prashant Meena Grasis</i> | 19 - 30 |
| 4       | Development and Validation of an HPTLC Method for Qualitative and Quantitative Estimation of Quercetin in <i>Glinus oppositifolius</i> (L.)<br><i>-Tushar Adhikari, Prerona Saha</i>  | 31 - 43 |
| 5       | <i>Madhuca longifolia</i> leaf extract mediated synthesis of ZnO nanoparticles and their Antibacterial, Antioxidant, and Photocatalytic activity<br><i>-Rajani1, Rishi Kesh Meena2, Preeti Mishra2</i>  | 44 - 56 |



---

---

# Development and Validation of a simple UV spectrophotometric method

**Vaishali Pardeshi\*, Tushar Lokhande , Rina Firke , Sneha Patil , Vishakha Pawar**  
Department of Pharmaceutical Chemistry, Mahatma Gandhi Vidyamandir's Pharmacy College,

## **ABSTRACT**

*Using a Shimadzu UV-2600, a quick, precise, easy, and affordable UV spectrophotometric approach has been created. Solvent made with methanol to assess the bulk Delamanid content. A wavelength of 320 nm was used for the detection process. The parameters linearity, accuracy, precision, ruggedness, robustness, LOD, and LOQ were taken into consideration during method validation in accordance with ICH Q2R1 criteria. It demonstrated linearity in the range of 60-360 ( $\mu\text{g/mL}$ ) at a predetermined  $\lambda_{\text{max}}$  of 320 nm, and it had a strong correlation coefficient ( $R^2=0.996$ ) and outstanding mean recovery (99.00-100.07%). Determination of Delamanid used this technique effectively. The method's linearity, accuracy, repeatability, and reproducibility were statistically and by recovery experiments confirmed. The outcomes demonstrated the method's applicability for both regular Delamanid bulk analysis and commercial formulations.*

**Keywords:** Delamanid, UV Spectrophotometric method, Process validation, ICH guidelines

## **INTRODUCTION**

The drug delamanid is efficient in treating MDR TB. It is referred to by its trademark, Deltyba. 1. It is the first of a brand-new class of anti-TB drugs known as nitroimidazoles [1]. The chemical name for delamanid is (2R)-2-[(4-(trifluoromethoxy)phenoxy)-(1-piperidinyl)]-6-nitro-2-[(4-(trifluoromethoxy)phenoxy)methyl].

Dihydroimidazo[2,1-b] [2, 3] oxazole as shown in Figure 1. Delamanid is a medication used to treat individuals with multidrug-resistant tuberculosis (TB) that affects the lungs. By preventing the production of mycobacterial cell wall constituents such as methoxy mycolic acid and ketomycolic acid, it functions as a prodrug [1, 2]. For delamanid's analysis, no spectroscopic, HPLC, or HPTLC approach is available. thus Delamanid's analytical procedure needs to be developed. The current study's objective was to create a precise, repeatable, accurate UV approach for the analysis of delamanid. The developed method looked for linearity, accuracy, precision, robustness, ruggedness, LOD, and LOQ in accordance with ICH guidelines [4].

It is branded as Deltyba 50mg available in tablet form. Methanol, DMSO (Dimethyl Sulfoxide), and DMF are all solubilizing solvents for it. Keto mycolic acid and methoxy mycolic acid, two crucial mycolic acid constituents, have been demonstrated to be prevented by delamanid. Delamanid's inhibitory effect is restricted to mycobacteria since mycolic acids are only present in the cell walls of mycobacteria and are not present in the cell walls of other Gram positive or Gram-negative bacteria [3,

5]. Breaking the cell wall enables increased medication penetration and hence a shorter treatment schedule since these acids make it harder for pharmaceuticals to

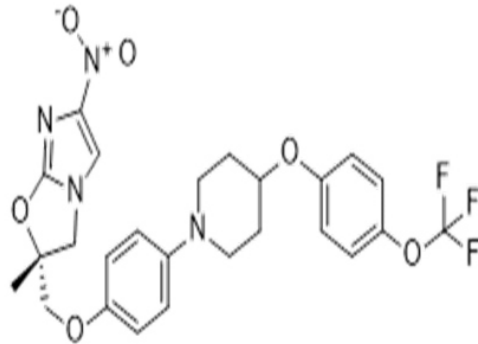


**Figure 1: Delamanid**

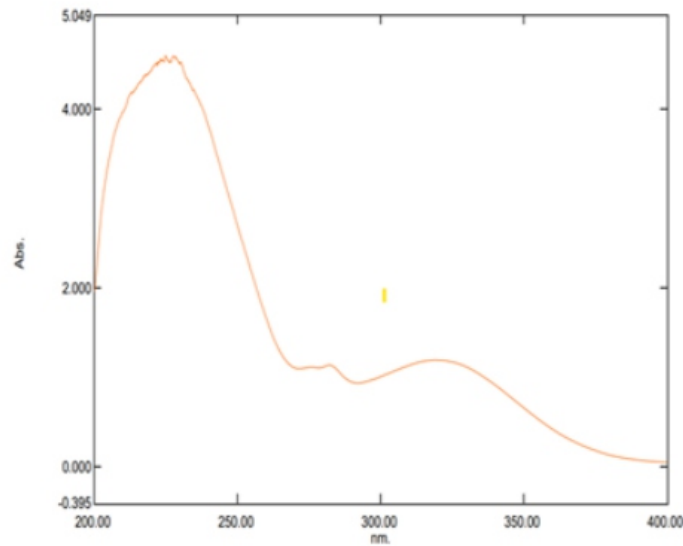


**Figure 2: UV spectra showing Absorption Maxima ( $\lambda$  max) of Delamanid**

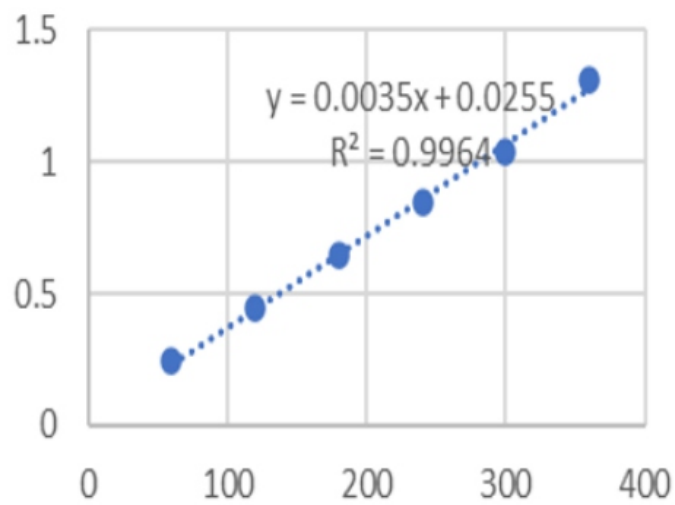


**Figure 3: Calibration Curve of Delamanid**

permeate the mycobacterium's cell wall [6, 7].



---

---

## MATERIALS AND METHODS

Delamanid pure drug was received as a gift sample from Mylan, Hyderabad. Analytical grade Ethylacetate, methanol and n-hexane were acquired from Qualigen (India) Ltd., Mumbai, India. All other chemicals come from S.D. Fine Chemical Ltd. in Worli, India, and are of analytical quality and for all of the experimental work, volumetric glassware of class A grade was employed. On a SCHIMADZU 2600 Double Beam UV-Visible Spectrophotometer with two 10 mm matched quartz cells, the UV spectrophotometric technique was used.

Solvents such as methanol, ethanol, toluene, petroleum ether, acetonitrile, chloroform, n-hexane and acetone were tried for the estimation of Delamanid. Because of easy availability, better solubility and cost effectiveness. Methanol was chosen as the solvent for the Delamanid analysis

**Table 1: Calibration Parameters**

| Sl.No. | Concentration ( $\mu\text{g/mL}$ ) | Absorbance |
|--------|------------------------------------|------------|
| 1      | 60                                 | 0.247      |
| 2      | 120                                | 0.447      |
| 3      | 180                                | 0.646      |
| 4      | 240                                | 0.845      |
| 5      | 300                                | 1.038      |
| 6      | 360                                | 1.314      |

### Standard Stock Solution Preparation

Delamanid was carefully measured at 50 mg and added to the volumetric flask at 50 ml. Prepared up to 50 ml with the same after being dissolved in a small amount of methanol to obtain a concentration of 1000 /ml(1000 ppm). 3.6 ml of the stock solution was transferred into a 10 ml volumetric flask and diluted with methanol. The dilution was observed to contain 360 $\mu\text{g/ml}$ .

### Determination of Wavelength of Maximum Absorption

Using methanol as a blank, the 360 g/ ml concentration solution was scanned between 200 and 400 nm. (Figure 2 )  $\lambda_{\text{max}}$  was determined to be 320 nm from the UV spectra and was chosen as the analytical wavelength. The UV spectrum of Delamanid was shown in Figure 2.

### Preparation of Calibration Graph

In this method, 0.6-3.6 ml of the aliquots of stock solution of Delamanid containing 1000 $\mu\text{g/ml}$  were transferred into six 10 ml volumetric flasks in a sequence. (60 - 360  $\mu\text{g/ml}$ ) and made up to the volume with methanol.

At 320 nm, the absorbance of solutions of various concentrations was measured in comparison to a

blank. By graphing concentration vs absorbance, the calibration curve was created.

At 320 nm, it was discovered that the sample was linear with a concentration range of 60 to 360 µg / ml.

**Table 2: Recovery study**

| Drug      | Initial amount Standard drug(100ppm) % | Amount added (200ppm) | Amount found | Recovery (%) | % RSD (n = 3) |
|-----------|--|-----------------------|--------------|--------------|---------------|
| Delamanid | 80%(10ppm)                             | 180ppm                | 181.2        | 101.2        | 0.07          |
|           | 100%(10ppm)                            | 200ppm                | 197.3        | 98.9         | 0.2           |
|           | 120%(10ppm)                            | 220ppm                | 218.6        | 99.3         | 0.3           |

**Table 3: Precision**

| Drug      | Con. (µg/ml) | Absorbance measured Mean ± SD % | Intra - Day |                   |             | Inter - Day |     |                   |
|-----------|--------------|---------------------------------|-------------|-------------------|-------------|-------------|-----|-------------------|
|           |              |                                 | RSD         | Average Potency % | Mean SD     | ±           | RSD | Average Potency % |
| Delamanid | 120          | 0.455±0.005                     | 1.1         | 104               | 0.462±0.002 | 0.6         |     | 103.4             |
|           | 180          | 0.648±0.006                     | 1.1         | 100.1             | 0.66±0.003  | 0.5         |     | 100.7             |
|           | 240          | 0.842±0.004                     | 0.45        | 100.8             | 0.851±0.006 | 0.14        |     | 98.2              |
|           |              | Mean RSD                        | 0.8         |                   |             |             | 0.4 |                   |

## Validation of Developed UV Spectrophotometric Method

### Linearity

A calibration graph was created between concentration and absorbance. With a concentration range of 60–360 µg / ml at 320 nm, delamanid was linear. Additionally, the assay's limit of quantitation (LOQ) and limit of detection (LOD) were determined.

### Precision

By conducting intra-day and inter-day variation trials using just three concentrations of Delamanid (120, 180, and 240 ppm) nine times, the suggested method's accuracy was evaluated. Intra-day studies and inter-day studies were determined by analysing three sample solutions of concentrations 120,180,240. The mean, standard deviation and % RSD were calculated.

### Accuracy (Recovery Studies)

A blend of pure Delamanid and common excipients were used in this investigation. Calculations were made using the label claim and the typical final product weight.

The admixture was diluted using the same method as before to achieve three concentrations: 80%, 100%, and 120% of the reference solution. By incorporating a known quantity of the sample solution into the standard stock solution, the investigation was carried out.

### LOD and LOQ

The set of six calibration curves used to assess the method's linearity was utilised to estimate  $LOD=3.3/S$  and  $LOQ=10/S$  Where  $\sigma$  is the standard deviation of the regression line's y-intercepts, The calibration curve's slope is denoted by S.

### Ruggedness

The degree of repeatability of outcomes under various settings is known as ruggedness. Delamanid's decision to switch the analyst proved the robustness of the process.

The method's ruggedness was found by changing the analyst. The findings of the statistical analysis of the data are given as mean, standard deviation, and percent RSD.

**Table 4: LOD and LOQ**

| Drug      | LOD     | LOQ      |
|-----------|---------|----------|
| Delamanid | 22.9ppm | 69.54ppm |

### Robustness

For determination of the robustness of the method, wavelength change was applied as  $\pm 2$  nm.

Following the statistical analysis of the data, the results are presented as mean, standard deviation, and % RSD

**Table 5: Ruggedness**

| Drug Concentration (ppm) | Analyst-1       |               |             | Analyst-2       |               |             |
|--------------------------|-----------------|---------------|-------------|-----------------|---------------|-------------|
|                          | Mean Absorbance | %Amount found | % RSD (n=3) | Mean Absorbance | %Amount found | % RSD (n=3) |
| 120                      | 0.447           | 102           | 0.8         | 0.440           | 98.7          | 0.3         |
| 180                      | 0.646           | 100.6         | 0.4         | 0.651           | 97.7          | 0.5         |
| 240                      | 0.845           | 101.5         | 0.7         | 0.858           | 99.10         | 0.3         |

**Table 6: Robustness data of UV-Vis spectrophotometric method by taking absorbance at  $320\pm 2$ nm**

| Sl. No | Concentration (ppm) | 318nm | 320nm | 322nm | %Amount | %RSD |
|--------|---------------------|-------|-------|-------|---------|------|
| 1      | 120                 | 0.436 | 0.438 | 0.437 | 97.9    | 0.2  |
| 2      | 180                 | 0.660 | 0.661 | 0.665 | 101     | 0.3  |
| 3      | 240                 | 0.868 | 0.860 | 0.865 | 99.9    | 0.4  |

---

---

## RESULTS AND DISCUSSION

### Method Development and Validation

Delamanid is easily soluble in organic solvents including methanol, DMF, and DMSO but practically insoluble in aqueous media. A few millilitres of methanol used as the diluent during the development phase produced a more favourable UV analysis result. The predetermined maximum absorption wavelength ( $\lambda_{\max}$ ) was 320 nm.

### Method Validation

#### Linearity

It was discovered that the calibration curve exhibits linearity in the range of 60-360  $\mu\text{g/ml}$  with a regression coefficient of 0.996 (Figure 3). With a correlation coefficient ( $r$ ) of 0.996, the equation  $y = 0.0035 + 0.0255x$  was produced via linear regression of absorbance on concentration. The maximal wavelength at 320 nm is visible for the detecting wavelength.

#### Accuracy (Recovery Studies)

RSD and the percentage recovery were computed. The present study work is correct in the technique creation of Delamanid since the mean percentage recovery and RSD were discovered to be within limits and less than 2. Calculations were made to determine the mean, standard deviation, and percentage relative standard deviation (%RSD). Table 2 presented the outcomes.

#### Precision

The repeatability (intraday) and intermediate precision (inter-day) of the assay were used to calculate its precision, which was reported as RSD%. For this, 120  $\mu\text{g/mL}$ , 180  $\mu\text{g/mL}$  and 240  $\mu\text{g/mL}$  concentration solution were measured three times a day and RSD% was calculated. (Table 3). In terms of intra- and inter-day precision, Delamanid's % RSD was discovered to be 0.6366 and 0.666, respectively. Table 3 displayed the results for intra-day and inter day. The devised technique's intra-day and inter-day precision study (Table 1), where all the RSDs were 2%, demonstrated appropriate sample stability and method dependability.

#### LOD and LOQ

Limit of Detection (LOD) and Limit of Quantitation (LOQ) estimates were used to determine the suggested method's sensitivity. Results are shown in Table 4.

#### Ruggedness

---

---

Table 5 displays the results for toughness. The method's robustness is demonstrated by the low percentage RSD value

### **Robustness**

A slight planned modification in the analytical wavelength proved the method's robustness. The wavelength change applied as  $\pm 2$  nm. At the selected variable wavelength, the amount of formulation was found. The % RSD was found to be 0.15, 0.36, 0.10 for variables shown in Table 6.

### **CONCLUSION**

The proposed UV-Vis Spectrophotometric approach was validated in accordance with ICH requirements and proved to be quick and accurate for estimating Delamanid. Therefore, without interfering with routinely used excipients, this method can be quickly and conveniently employed for routine analysis of Delamanid in quality control laboratories, whether in bulk or dosage formulations.

### **ACKNOWLEDGMENT**

For giving a gift sample, the authors are grateful to Mylan Lab in Hyderabad, India. Also grateful for the facilities provided for doing this study work by the Principal of Mahatma Gandhi Vidyamandir's Pharmacy College Panchavati Nashik.

### **Funding Support**

The authors declare that they have no funding support for this study.

### **Conflict of Interest**

The authors declare that they have no conflict of interest.

### **REFERENCES**

- [1] A Bahuguna and D S Rawat. An overview of new antitubercular drugs, drug candidates, and their targets. *Medicinal Research Reviews*, 40(1):263–292, 2020.
- [2] S K Field, D Fisher, J M Jarand, and R L Cowie. New treatment options for multidrug-resistant tuberculosis. *The Adv Respir Dis*, 6(5):255–268, 2012.
- [3] M Matsumoto, H Hashizume, and T Tomishige. OPC-67683, a nitro-dihydro-imidazooxazole derivative with promising action against tuberculosis in vitro and mice. *PLOS Med*, 3(11):2131–2144, 2006.
- [4] Validation of analytical procedure: text and methodology. *International Conference on Harmonizations*, pages 1–17, 2005.

---

---

[5] *MS Glickman and W R Jacobs. Microbial pathogenesis of Mycobacterium tuberculosis: dawn of a discipline. Cell, 104(4):236–243, 2001.*

[6] *Stephen K Field. Safety and Efficacy of Delamanid in the Treatment of Multidrug-Resistant Tuberculosis. Clinical medicine insight: therapeutics, 5(5):137–149, 2013.*

[7] *J Nicola, Jin Han Ryan, and Lo. Delamanid: first global approval. Drugs, 74(9):1041–1045, 2014.*

---

---

# Diagnostic Aids and Techniques of Oral Cancer- An Updated

Deivanayagi M1 , Afreen Fathima I\*2

1Department of Oral Medicine and Radiology, Adhiparasakthi Dental College and Hospital, Melmaruvathur - 603319, Chengalpattu, Tamil Nadu, India

2Ragas Dental College and Hospital, Uthandi- 600119, Chennai, Tamil Nadu, India

## **ABSTRACT**

*Oral cancer is the most prevalent and lethal type with a four in every 3000 incidence rate worldwide and a 3% survival rate. Oral squamous cell carcinoma (OSCC), which is multifactorial, is brought on by genetic and epigenetic instability. Oral potentially malignant disorders (OPMDs) are precursor lesions that often precede oral cancer, and their early diagnosis is advantageous for patients since it may lengthen their productive longevity. Currently, oral cancer screening, early identification, and its pre-invasive intraepithelial phases are still largely focused on visual inspection of the mouth. These methods are subjective and early lesions can be easily missed. Due to a lack of early identification, oral cancer's five-year survival rate is still low. Recently, the World Health Organization (WHO) and the International Agency for Research on Cancer (IARC) emphasised that by developing efficient cancer control and screening strategies, we can prevent a third of the 15 million cancer cases that are expected to occur in the future and better manage a second third. Oral cancer screening aids and techniques have witnessed a lot of advancements recently. This article reviews the current diagnostic methods and instruments for detecting oral cancer, which include the oral CDx brush, Velscope, Chemiluminescence, DNA ploidy, microarray technology, colposcopy, and oral scan. It also adds on the molecular (genetic and epigenetic alterations) & decoding of the oral carcinogenesis genomics data.*

**Keywords:** Delamanid, UV Spectrophotometric method, Process validation, ICH guidelines

## **INTRODUCTION**

Due to its high rates of morbidity and mortality, oral cancer—a disease that affects everyone—has developed a reputation for being difficult to treat [1].

Approximately 643 000 new cases of head and neck cancer (H&N cancer), which includes all oral, laryngeal, and pharyngeal sites, are diagnosed each year [2]. The greater morbidity linked to this fatal disease is attributable to the disease's delayed diagnosis and advanced stage presentation [1]. Preventing oral cancer and detecting it early are two key goals in reducing its prevalence worldwide, according to the World Health Organization [2].

### **Diagnostic Aids, Techniques & Recent Advances Cytopathologic Studies Brush biopsy**

It is sometimes referred to as the OralCDx Brush Test system, which is a technique for obtaining a sample from the lesion of the mucosa of the trans-epithelial cell that represents the basal, parabasal, and superficial layers of the epithelium. Due to its low-risk clinical characteristics, this test was created primarily to look at abnormalities in the mucosa that usually do not necessarily require a biopsy. Samples of epithelial cells are smeared on a glass slide, which is then prepared for a modified form of the Papanicolaou test, and it is assessed via a microscope. A brush that is specifically made is used as the device

---

---

without causing any laceration for collecting cells of the epithelium [2].

### **Liquid based cytology with Oral CDx brush**

A dedicated oral tool (such as a CDx brush) has never been used in any liquid-based cytology research in the oral cavity; instead, sample collection has always been done using cervical or dermatological techniques. Inadequate results are anticipated since cervical brushes are not stiff [3]. An accuracy of 92.3 percent was found in a study by Mozafari et al with oral CDx brush, this may help to improve sensitivity and alleviate the issue of false negative and subpar outcomes [4, 5].

### **Light Based System**

#### **Chemluminescence (Reflective tissue fluorescence)**

The chemiluminescence method involves rinsing the mouth with one percent acetic acid, thereby helping to clear away debris and making epithelial cell nuclei more visible because of minor cellular dehydration [6]. The aberrant tissue will reflect the blue-white illumination, allowing the occult lesion (aceto-white & reflect light) to be distinguished from healthy mucosa (blue) [7].

#### **Tissue fluorescence imaging (Velscope System)**

A strong blue excitation light (400-460 nm) is used in this technique to illuminate the oral mucosa. This causes the aberrant tissue to glow as a result of altered epithelial and subepithelial stromal structure and metabolism [8]. Healthy mucosa displays an autofluorescence that is pale green, whereas the aberrant tissue tends to appear darker when compared to the normal tissue surrounding it [9]. According to case studies, the veloscope (Figure 1) has a high sensitivity (98–100%) and selectivity (3–100%) to identify the areas that have beyond changes of dysplasia and cancers that have expanded lesions that are clinically visible [7].

#### **Tissue fluorescence spectroscopy**

A spectrograph is used in this technique to gather, record and analyse the spectrum of the tissue's fluorescence that is reflected. A tiny optical fibre produces a variety of wavelengths that are excitation [10]. Technology distinguishes malignant tumours from healthy oral mucosa with accuracy





**Figure 1: Velscope& Detection of oral cancer by Velscope**

and success. Because the optical fibre can only assess a small area of the mucosa, spectroscopy is only used to assess well-defined small mucosal lesions that have already been diagnosed through clinical inspection to determine whether they are benign or (pre) malignant [11]. This technique is therefore unsuitable to detect lesions that are new or to assess larger lesions [8].

### **Oral scan**

An optical imaging multimodal tool called Oral Scan is used to find (pre-)cancerous lesions in the oral cavity as early as possible. The oral scan (Figure 2) system functions according to the diffuse reflectance and tissue autofluorescence theories, in which light is repeatedly absorbed and scattered before emerging from the tissue surface. Optical signals coming from tumour tissues are altered by the biochemical and morphological changes that occur during the carcinogenesis process.

Before taking a biopsy, the doctor can use OralScan to visualise and distinguish between healthy and potentially cancerous oral cavity regions. It is not an invasive procedure, the procedure is done in vivo, it images a very large field by using a cloud based machine learning algorithm to obtain results on the status of tissue and applies oxygenated hemoglobin (HbO<sub>2</sub>) absorption maps to guide the biopsy. All of these Oral Scans' diagnostic applications can be very beneficial in cancer diagnosis [12].

### **DNA Ploidy**

The amount of nuclear DNA is gauged by DNA ploidy. Feulgen dye-stained cytological samples are collated into an instance set of cells and analysed via computer to spot variations in cellular DNA concentration. Genomic instability contributes to cancer growth, and aberrant DNA content distinguishes dysplastic lesions from other cancers [5].



2.a

2.b.

**Figure 2: Oral Scan**

### **Microarray technology**

An array of DNA spots on a solid surface is represented by a DNA microarray. Utilizing this method, researchers may examine how different genes are expressed in diverse cancer types. A stand-in marker for this is messenger RNA (mRNA). In this approach, multitudes of oligonucleotides or fragments of DNA get covalently bonded onto a chip (solid surface) and arranged in rows and columns in a predefined sequence in either a 2D or 3D configuration. Reverse transcription and labelling of the sample RNA would enable the identification and quantification of particular transcripts. Restriction endonucleases are used in the microarray approach to cut unknown DNA segments, allowing fluorescent markers to respond to chip probes of DNA. The probes cohere with the DNA fragments. Fluorescence emission enables a recognition of the target DNA pieces. The examination of numerous molecular markers from a sample of one patient is made easier by gene expression arrays. Microarrays are used in OSCC to identify single nucleotide polymorphisms (SNPs), gene mutations, cancer biomarkers, and genes involved in drug discovery and chemoresistance [1].

### **Next-generation sequencing**

Sanger sequencing was used to sequence the first piece of DNA in 1977. Second-generation sequencing was first launched in 2005. DNA extraction with the rapid gathering of extensive sequencing data is made possible by NGS technologies. Furthermore, NGS techniques provide an important understanding of genetic paths, allowing us to comprehend the onset and progression of the disease. Various NGS techniques can be used for DNA sequencing, whole genome characterisation, coding genome analysis, copy number checks, translocation detection, and mRNA abundance assessment. The Illumina/Solexa Genome Analyzer, Roche/454 FLX, the Helixos Heliscope™, Life Technologies Ion Torrent, and other NGS systems are commercially available.

---

---

Third-generation sequencing (TGS) has recently been made available using one molecule. NGS systems have made it possible for us to comprehend the numerous genomic changes found in OSCC [1].

### **Colposcopy (direct microscopy)**

Colposcopy is a well-known procedure of diagnosis that is implemented to examine vaginal, vulvar, and cervix tissues while illuminating the area of interest with a magnified view. When using a portable video camera attached to a colposcopy device, it is possible to observe three-dimensional images of the tissue surfaces being inspected on a television monitor. White or yellow light, which is unfiltered, blurs the distinction between arterioles and surrounding tissue, so the colposcope is equipped with a blue or green filter to authorize the evaluation of changes in vascularity and colour quality. The ideal working distance for the microscope's focal length is 200 mm. According to a study, colposcopy done on premalignant lesions of the mouth was accurate in identifying oral mucosal abnormalities in the range of 70% to 98 percent [10].

### **Salivary Biomarkers**

Over a hundred possible biomarkers of the oral cavity have been identified in the English literature, mostly based on comparisons between the amounts found in patients with the disease and those found in healthy individuals serving as controls. A number of salivary proteins have been studied, including  $\alpha$ -amylase, interleukin 8, tumour necrosis factor  $\alpha$ , Statherin, CA 125, Endothelin-1, CD44, Catalase, Cyclin D1, and CEA. The few difficulties in using this technique include the lack of valuation for the technique of collecting samples of saliva [10].

### **Cell and tissue markers**

Epithelial growth factor (EGF), Cyclins, AgNOR, bcl2, and telomerase have all been employed as tumour growth markers [23]. Four hypoxia biomarkers— GLUT-1, carbonic anhydrase IX, hypoxia inducible factor 1 $\alpha$ , and erythropoietin receptor—as well as three angiogenic biomarkers—CD105 and Eph receptor tyrosine kinases (Ephs), vascular EGF, have been found as biomarkers. Tumour suppression markers and an anti-tumor response include retinoblastoma protein, p53, and cyclin-dependent kinase inhibitors. The matrix metalloproteins are proteases that are frequently evaluated in various research, and they are commonly expressed by invasive tumours and adjacent stroma. Desmoplakin, Integrins, and cathepsins have all been identified as indicators of tumour invasion. Investigations have been done on cytokeratins, filaggrin, involucrin, and glutathione S-transferase [10].

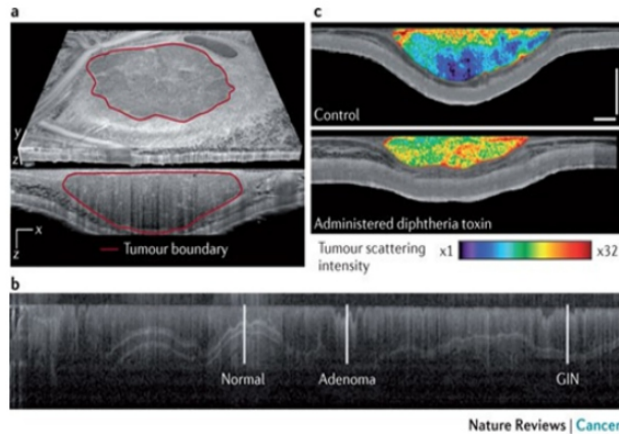


**Figure 3: Optical coherence tomography revealing tumor**

### Elastography

One important factor used to distinguish an enlargement that is inflammatory and malignant is the hardness (elasticity) of the lymph nodes. Elastography evaluates the cellular structure's compliance behaviours. Tissue hardness can be calculated by measuring the displacement or strain that tissue compression causes in the tissue's structural elements. The elastography images are compared before and after cervical lymph node compression [10].

### Surface enhanced Raman spectroscopy

This method provides a precise, highly accurate acquisition of the structure of the molecular tissue because of the unique way that biological molecules interact with photons. Lipid, nucleic acid, and protein spectral characteristics serve as accurate Raman indicators to distinguish between cancerous and healthy oral mucosal tissue. Raman spectroscopy contributes knowledge that is comparable to or even superior to established methods in oral carcinogenesis. The drawbacks include a lack of spatial information, intensive processing, expensive equipment requirements, randomness, nonimaging, and complex algorithms to separate different tissue classifications [10].

### Positron Emission Tomography

The fluorodeoxyglucose-positron emission tomography (FDG-PET) test exhibits excellent prognostic precision and importance in characterising lymphatic status, aiding in the analysis along with prompt identification of cancer of the oral cavity. PET or computed tomography (CT) could detect as well as differentiate persistent or recurrent neoplasias from surgical or radiation-induced alterations because malignant cells contain an increased amount of FDG for a lot of time when compared to infectious and inflamed structures. According to recent studies, PET/CT was highly accurate (> 90%) at finding the recurrent tumour [10].

---

---

## Optical coherence tomography

A minimally invasive tomographic imaging technique is optical coherence tomography (OCT). The method creates a cross-sectional architectural representation of the tissue using subsurface reflections to identify areas of inflammation, dysplasia, and malignancy. The oral mucosa can be imaged using OCT technology with insertion into the tissue up to one to two mm deep [4]. Optical coherence tomography involves capturing below the surface pictures to provide a comprehensive cross-sectional picture (Figure 3). The difference between in-vivo images of malignant lesions of the oral cavity in a hamster is enhanced by the multimedia dispersion of polyethylene glycol that is connected to gold nanoparticles attached to antibodies. A recent pilot study involving 27 cancer patients revealed the viability of using optical coherence tomography to find structural alterations in malignant molecules [10].

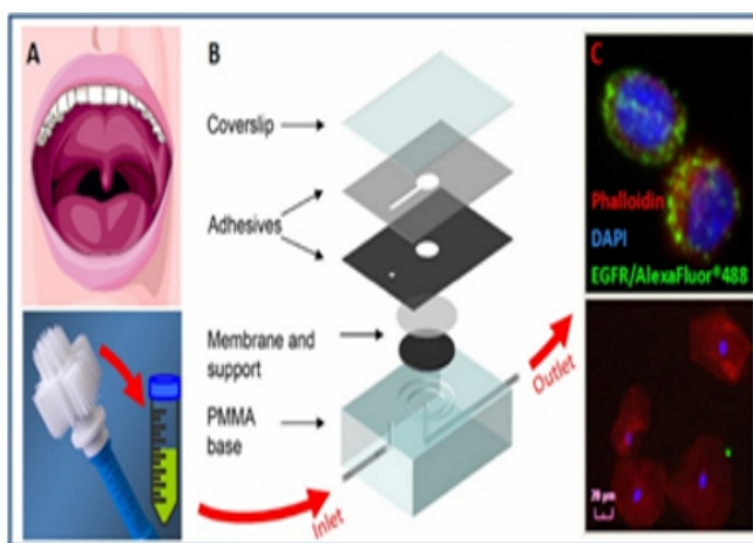


**Figure 4: Bio nano-chip**

Highly accurate, yet user friendly, inexpensive and non-invasive technology for detecting oral cancer in resource-constrained clinical settings has been developed by Scientists at IIT Kharagpur (Indian institute of technology) which is based on OCT.

This diagnostic device is a portable and easy to operate blood perfusion imager (BPI) along with a miniature far-infrared (FIR) camera and a humidity sensor, which have been controlled via electronic as well interfaced along merge with physics-based and a software engine that is driven by data.

The actual gadget is made up of a probing unit to screen and a processing unit to gather information about blood perfusion along with diagnosing diseases. The sensor housing and holder that make up the probing unit keep the sensors in a stable environment while minimising the effects of breathing. The utility of the holder is to guide sensor housing towards the site of measurement. Sensor housing comprises a digital humidity sensor that is completely computed for detecting the ambient temperature and relative humidity in the oral cavity, as well as an on-chip long-wave infrared (IR) camera for measuring the temperature of the tissue. Using additional signal-processing electronics, the IR camera sensor array

---

---

converts into temperature values, the radiometric values alongside thermal sensitivity 50 mK (milli Kelvin). The imaging occurs at a rate of 8.7 Hz, capturing spectral illumination in the wavelength range of 8 to 14 m (micrometre).

## Bio-Nanochip

A novel bio-nanochip (BNC) (Figure 4) sensor was recently documented. It is quite a quick cytology test of the oral cavity that combines the benefit of cytological morphometric analysis alongside the quantification of neoplastic biomarkers. Microfluidics technology, sometimes known as "lab-on-a-chip," is generally defined as the adaptation, miniaturisation, fusion, and automation of analytical laboratory techniques into a single chip. The BNC sensor used membrane-related cell proteins, which are particularly prevalent in the cellular membrane structure of malignant cells, to identify cancerous cells [10].

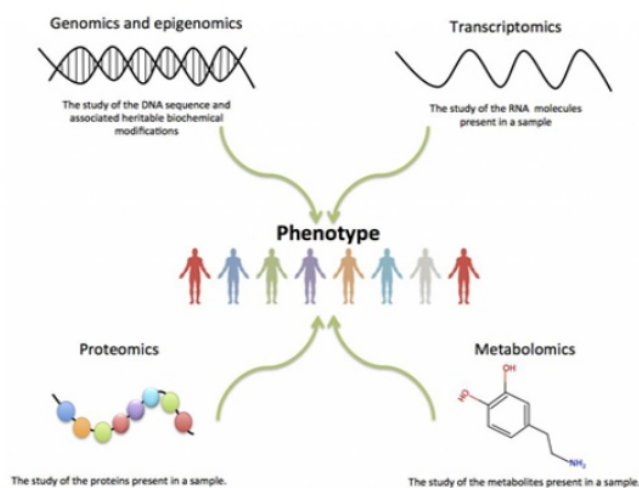


**Figure 5: Genomics, proteomics, transcriptomics**

## PCR-Based diagnostic aids

Polymerase chain reaction (PCR) can be used to examine and diagnose infectious diseases and cancers linked to microbes. PCR is a crucial method for detecting mutations occurring in cancer-related oncogenes (such as K-ras and N-ras), tumour suppressing genes (such as p53 and p16), and other genes. The PCR technology has expanded the scope and diagnostic technique sensitivity, however, there is still a significant downside, due to the possibility that contamination and amplification artefacts could make it difficult to understand the required results. PCR, reverse transcriptase PCR (RT-PCR), and various molecular techniques have made it possible to diagnose and predict the prognosis in additional lesions, like chronic myelogenous leukaemia [11].

## "Omics" in oral cancer

By decoding oral carcinogenesis, genomics data considerably improve our knowledge and understanding, which in turn aids in the development of targeted treatments and prognosis prediction. In order to

---

---

finally improve the lives of OSCC patients, high-throughput technology is being applied to give insight into the underlying molecular pathways (genetic and epigenetic alterations) in OSCC [1].

### **Genomics**

Genomic profiling (Fig 5) of OSCC is essential taking into account the inter-tumor and intra-tumor heterogeneity. Various alterations in the chromosome are reported in OSCC for instance, loss at 3p and WISP1 genes. Recently, core dysregulated pathway and target that is actionable are identified, which might dictate the use of more involved and affordable sequencing panels [1].

### **Transcriptomics**

By using the high-throughput technique, transcriptomics concerns to study of transcriptome, that is the absolute set of RNA transcripts made by the genome under specified conditions [1].

### **Proteomics**

Proteomics (Figure 5) is the study of the full range of proteins expressed in an animal's tissues. Due to a large number of OSCC biomarkers currently in use, non-invasive samples including blood, serum, and various other bodily fluids have a benefit over tissue samples [1].

### **Synthetic biology**

Principles of synthetic biology are being investigated in the areas of genetic engineering, genome editing, and cancer immunotherapy. In order to modify the biological environment (by creating chimeric antigen receptors), and create synthetic oscillators, thereby changing the genome, synthetic biology has been expanded. It has been suggested that use synthetic networks as a cancer treatment technique. For instance, a microRNA-based cancer cell classifier makes use of microRNA expression to detect cancer cells and then initiate apoptosis.

The Clustered Regularly Interspaced Short Palindromic Repeats (CRISPR) system for genome editing was formerly assumed to be the bacteria's developed resistance to viruses and plasmids. CRISPR is effective, simple to use, and commonly used in genome editing techniques [1].

### **CONCLUSION**

The WHO has insisted on focusing majorly upon early diagnosis to reduce the number of deaths due to cancer, and there are a lot of developments since the last decade. Advanced, non-invasive and accurate devices or methods are the only hope to prevent cancer related deaths among the public. Early diagnosing gives a better prognosis, and it is important for a clinician to be up-to-date with such advancements for the betterment.

---

---

## Funding Support

The authors declare that they have no funding support for this study.

## Conflict of Interest

The authors declare that they have no conflict of interest.

## REFERENCES

- [1] MG Madhura, RS Rao, S Patil, HN Fageeh, A Alhazmi, and KH Awan. *Advanced diagnostic aids for oral cancer. Disease-a-Month*, 66(12), 2020.
- [2] Stefano Fedele. *Diagnostic aids in the screening of oral cancer. Head & Neck Oncology*, 1(5):1–6, 2009.
- [3] M Sarah Freygang, R Grasieli De Oliveira, R Elena Riet Correa, M Filipe, and G Liliane Janete. *Techniques for Precancerous Lesion Diagnosis. Journal of Oncology*, pages 1–5, 2011.
- [4] Zahra Pegah Mosannen Mozafari, Nooshin Delavarian, and Mohtasham. *Diagnostic Aids in Oral Cancer Screening. Oral and Maxillofacial Diseases Research Center*, pages 189–208, 2011.
- [5] TC Folsom, CP White, L Bromer, HF Canby, and GE Garrington. *Oral exfoliative study: Review of the literature and report of a three year study. Oral Surgery, Oral Medicine, Oral Pathology*, 33(1):61–74, 1972.
- [6] R Navone, P Burlo, A Pich, M Pentenero, R Broccoletti, A Marsico, and S Gandolfo. *The impact of liquid based oral cytology on the diagnosis of oral squamous dysplasia and carcinoma. Cytopathology*, 18(6):356–360, 2017.
- [7] MW Lingen, JR Kalmar, T Karrison, and P M Speight. *Critical evaluation of diagnostic aids for the detection of oral cancer. Oral oncology*, 44(1):10–22, 2008.
- [8] S Shamimul Hasan and Elongovan. *Conventional and Advanced Diagnostic aids in Oral Cancer screening - The journey so far. International Journal of Pharmacy and Pharmaceutical Sciences*, 7(1):29–33, 2014.
- [9] N Mohan, T Kumar, and Subbulakshmi. *Clinical Diagnostic Tools in Detection of Oral Cancers and Potentially Malignant Disorders. Journal of Medical Science and Clinical Research*, 5(2):17715–17720, 2017.
- [10] Gaurav Sharma. *Diagnostic aids in the detection of oral cancer: An update. World Journal of Stomatology*, 4(3):115–120, 2015.
- [11] M K Masthan, N A Babu, K C Dash, and M Elumalai. *Diagnostic Aids in Oral Cancer. Asian Pacific journal of cancer prevention*, 13(8):3573–3576, 2012.
- [12] Biospectrum. *Sascan meditoool launches hand held oral cancer screening tool. 2020. Accessed on: 23 October 2020.*



---

---

# Etiological Evaluation of Microcytic Hypochromic Anemia at a Tertiary Care Hospital in the Eastern Part of India

Prabhat Kumar<sup>1</sup>, Arun Kumar Singh<sup>1</sup>, Anju Bharti<sup>2</sup>, Sandeep Kumar<sup>1</sup>, Chanda Hemaliya<sup>3</sup>, Sandip Kumar<sup>2</sup>, Lalit Prashant Meena<sup>\*1</sup>

<sup>1</sup>Department of General Medicine, Institute of Medical Sciences, Banaras Hindu University, Varanasi, Uttar Pradesh, India

<sup>2</sup>Department of Pathology, Institute of Medical Sciences, Banaras Hindu University, Varanasi, Uttar Pradesh, India

<sup>3</sup>Institute of Medical Science, Banaras Hindu University, Varanasi, Uttar Pradesh, India

## **ABSTRACT**

*Microcytic hypochromic anemia is a part anemia classification based on the morphology of anemia with well-known causes and management. The causes of microcytic hypochromic anemia may be either due to iron deficiency anemia, anemia of inflammation, or thalassemia. There are lots of recent advancements and studies done on the etiology of Microcytic Hypochromic anemia but accurate data especially from the eastern part of India are not available. To investigate the causes of Microcytic Hypochromic anaemia at a tertiary care centre in eastern India. After obtaining valid written consent, cases of microcytic hypochromic anaemia were selected from the OPD and indoors for this cross-sectional investigation. The whole haematological and biochemical investigations were sent for anaemia workup. The study comprised 100 patients with microcytic hypochromic disorder. The study comprised subjects ranging in age from 18 to 80 years. 39% were men and 61% were women. In thalassemia patients, the most common were b-thalassemia traits in 81.8 %, followed by 9% of each Delta B-thalassemia and double heterozygous HBE and beta thalassemia. Anemia is not an illness in and of itself, but rather a symptom of another, hence finding the underlying cause is significantly more important. The diagnosis of microcytic hypochromic anaemia is insufficient in the absence of an underlying cause. Special precautions will be made to determine the cause of iron deficient anaemia. The thalassemia trait must also be diagnosed in order to minimise excessive iron supplementation and for family screening.*

**Keywords:** Iron-Deficiency Anemia, Anemia of Chronic Disease, Microcytic Hypochromic Anemia

## **INTRODUCTION**

Anemia is a disorder in which the amount of circulating red blood cells (RBC) or their oxygen-carrying ability is insufficient to meet a person's physiologic needs, which vary depending on age, gender, altitude, smoking, and pregnancy [1]. Anemia is a global health issue that affects people of all ages, particularly children, adolescents, women of reproductive age, and the elderly. Anemia affects one-third of the global population and is linked to decreased labour productivity, increased illness and death, and aberrant brain development. Anemia affects 1.62 billion people worldwide, accounting for 24.8% of the world's population [2]. Anemia is not equally distributed throughout the world; it is fivefold more common in underdeveloped geographies. According to the National Family Health Survey 5, which was conducted in India from 2019 to 2021, the biggest jump in anaemia was recorded among children aged 6-

---

---

59 months 67.1% (NFHS-5) from 58.6%. (NFHS-4, 2015-16). The data shows that the number was higher in rural India (68.3 per cent) as compared to the urban population of India (64.2 %). This is followed by anemia in females aged 15-19 years 59.1 % (NFHS-5) from 54.1 % (NFHS-4). In this group, the number was higher in rural areas (58.7 %) compared to urban India (54.1 %). The prevalence of anemia among men, the data show, was significantly lower compared to other groups: 25 percent in the age group of 15-49 and 31.1 percent in the age group of 15 years. A similar cross-sectional observational study was conducted on patients with microcytic hypochromic anaemia who attended the R G Kar medical college and hospital's medicine and paediatrician outdoor department using the following parameters: RBC indices (MCV, MCH, MCHC), RDW, Serum IRON, Serum FERRITIN, Total Iron Binding Capacity (TIBC), and High Performance liquid chromatography (HPLC). Iron replacement therapy is commonly started in many centers without properly investigating patients to determine the cause of anemia. It is very important to follow an orderly approach in microcytic hypochromic anemia patients to correctly diagnose the etiology. This iron deficiency anemia generally masks the underlying diseases especially the thalassemia trait which cannot be diagnosed even by higher investigations like Hb electrophoresis unless the iron deficiency is corrected before the electrophoresis [3, 4].

Iron deficiency anemia is the most common cause of microcytic hypochromic anemia worldwide, other causes may be anemia of inflammation, thalassemia, or sideroblastic anemia. Anemia of chronic inflammation (previously called anemia of chronic disease-ACD) is a condition that accompanies a specific underlying disease, in which there is a decrease in hemoglobin, hematocrit, and erythrocyte counts due to a complex process, usually initiated by cellular immunity mechanisms and pro-inflammatory cytokines and hepcidin [5]. It is very important to follow an orderly approach in microcytic hypochromic anemia patients to correctly diagnose the etiology.

In this study, we evaluate the etiology of microcytic hypochromic anemia in OPD and admitted patients at Sir Sunder Lal Hospital, Institute of Medical Sciences Banaras Hindu University, Varanasi.

### **Aims and Objective**

To evaluate the etiologies of Microcytic Hypochromic anemia at a tertiary care center in the eastern part of Uttar Pradesh of India.

## **MATERIAL AND METHODS**

### **Study Design**

This is a cross sectional study was carried out at a tertiary care hospital, from April 1st 2020 - July 31st 2021. Total 100 Cases of microcytic hypochromic anemias were taken from Outpatient Department and indoor. After taking written consent from all patients workup was done according to its etiology. The study was approved by the ethical committee of the institute.

---

---

## **Inclusion Criteria**

Age >18-year, Patient of microcytic hypochromic Anemia.

## **Exclusion Criteria**

Age <18 years, Patient who refuses to consent, Anemia not caused by microcytic hypochromic anaemia. Microcytic anaemia aetiologies are evaluated by sending complete haematological investigations such as complete blood count, reticulocyte count, peripheral blood smears, serum iron, total iron binding capacity (TIBC), ferritin, haemoglobin electrophoresis, LDH, stool for occult blood and ova, cysts, liver and renal function. Proctoscopy, anti-tissue transglutaminase/antigliadin antibody, upper GI endoscopy, lower GI endoscopy, bone marrow examination including iron staining, Xray, abdominal ultrasonography, computed tomography abdominal scans were performed on selected patients based on their symptoms.

## **Statistical Analysis**

The statistical analysis was performed using statistical package for the social sciences (SPSS), Version 23.0. IBM Corp., NY). Simple descriptive statistics was used (mean  $\pm$  standard deviation for quantitative variables, and frequency with percentage distribution for categorized variables). The statistical analysis was carried out for various categorical parameters using the chi-square test and Fischer's Exact Test. For comparing two groups of mean or median Student's t-test and Mann Whitney U test was performed. P-value <0.05 is considered as statistically significant.

## **RESULTS**

A total of 100 patients of microcytic hypochromic anemia were included in this study. Out of total 100 patients in this study, 44% were taken from OPD and 56% were from IPD. The selected population ranged in age from 18 to 80 years. The bulk of these 100 patients (26%) were between the ages of 61 and 70, while 22% were between the ages of 21 and 30. In this study, 61% of the patients were female, whereas 39% were male. The most prevalent presenting complaint was broad weakness and easy fatigability, which was reported by 96% of patients, followed by haemorrhoids (18%), fever (16%), melena, abdominal discomfort, and dyspnea on exertion (11%). Menorrhagia was found in 10% of female patients. In this study Digital rectal examination and Proctoscopy was done in 30 out of 100 patients, 18 patients (60%) had hemorrhoid, 40% had no abnormal findings. Out of total 18 hemorrhoid patients, 9 patients (50%) had grade -I, 6 patients(33.3%) had grade-II, 2 patients (5.5%) had grade -III, and 1 patient(5.5%) had grade-IV hemorrhoids. This study showed preponderance of microcytic hypochromic anemia in female patients (39% were male and 61% were females) and females were predominant in all age groups. In this study iron deficiency anemia was present more commonly in females (65.6%) than males (34.4%), anemia of chronic disease was present in 57% in males and 42.9%

---

---

in females and thalassemia was present in 18.2 % males and 81.8% in females.

In this study we observed that majority of patients (62%) had moderate anemia, Hemoglobin between 8-10gm/dl, 34% had severe anemia <8gm/dl and 4% patients had mild anemia hemoglobin >10 gm/dl. In this study out of total patients of micro cytic hypochromic anemia, the most common cause was iron deficiency anemia (61%), followed by anemia of chronic disease (28%) followed by thalassemia (11%) (Table 1). Lower gastrointestinal bleeding was the most common cause of iron deficiency anaemia in 34.4% of patients, followed by upper gastrointestinal bleeding (21.3%), menorrhagia (18% of total female count), pregnancy (9.8%), unclassified (4.9%), infectious (including hookworm in 4.9% and *Ascaris lumbricoides* in 1.6% of patients), chronic kidney disease (3.2%), and celiac disease (1.6%). Stool examination was performed on 73 individuals, with positive results for occult blood in 26 (35.6%), hookworm in 3 (4.1%), and *Ascaris lumbricoides* in one patient (1.3%), and negative results in 43 (58.9%). Distribution of iron deficiency anemia (IDA) according to different age group. Majority of the IDA is seen in elderly 61-70 year (32.7%) followed by reproductive age 21-30 years (21.3%) followed by 18% in age group of 51-60 year. Upper GI endoscopy and HPE (in selected individuals) were performed on 29 of 100 patients who had either occult blood in their stool or were suspected of upper GI bleeding. 15 of the 29 individuals had normal upper gastrointestinal endoscopies. Antral gastritis affected 13.7%, duodenal ulcers affected 10.3%, and gastroesophageal varices affected 6.8%. Other causes include sliding hiatus hernia with fundal gastritis, celiac disease, carcinoma stomach, NSAIDs induced gastritis and *Helicobacter pylori* induced gastritis. Only patients with no noteworthy findings on upper gastrointestinal endoscopy with stool for occult blood positive or suggestive of cancer underwent lower gastrointestinal endoscopy. Lower gastrointestinal endoscopy was performed on 9 patients, with no notable results on lower gastrointestinal endoscopy in three of them. 2 patients (22.2%) had grade I internal haemorrhoids, 1 patient (11.1%) had ulcerative colitis, 1 patient (11.1%) had Crohn disease, 1 patient had carcinoma colon (11.1%), and 1 patient (11.1%) had colonic diverticula. In this study, we observed that in patients of iron deficiency anemia, total 11 female patients had menorrhagia, out of these the most common cause was dysfunctional uterine bleeding in 6 patients (54.5%) followed by uterine fibroid in 2 patients (18.1%) and other causes includes 1 patient of uterine polyp, hypothyroidism and carcinoma cervix. In this study, we observed that anemia of chronic disease was the second most common cause of microcytic anemia after iron deficiency anemia. Out of total 28 AOCD patients, the most common cause was infection-Tuberculosis in 11 patients (39.2%) followed by chronic kidney disease in 3 patients(10.7%), followed by systemic lupus erythematosus in 3 patients (10.7%), next includes 2 patients from each of rheumatoid arthritis, multiple myeloma, diabetes mellitus and 1 patient of non Hodgkin lymphoma, Hodgkin lymphoma, Chronic lymphocytic leukemia, carcinoma lung and Crohn disease (Table 2). Distribution of anemia of chronic disease according to different age group. Majority of the AOCD is seen in older age groups as 21.4% in 41-50, 51-60 and 61-70 years of age followed by 31-40 year (17.8%), followed by 21-30 years age group (10.75%) In our study out of total

---

---

thalassemia patients most common was b-thalassemia trait in 81.8 %, followed by 9% of each Delta B – thalassemia and double heterozygote HBE and B thalassemia (Table 3). In our study, the demography of thalassemia patients were 4 patients (36.4%) were from

**Table 1: Etiological Distribution of Microcytic Hypochromic Anemia in Different Groups**

| Diagnosis                        | No. | %     |
|----------------------------------|-----|-------|
| Iron deficiency anemia (IDA)     | 61  | 61.0  |
| Anemia of chronic disease (AOCD) | 28  | 28.0  |
| Thalassemia                      | 11  | 11.0  |
| Total                            | 100 | 100.0 |

**Table 2: Etiology of Anemia of Chronic Disease**

| Etiology                     | No. | %        |
|------------------------------|-----|----------|
| Tuberculosis                 | 11  | 39.28571 |
| Chronic Kidney Disease       | 3   | 10.71429 |
| Systemic lupus erythematosus | 3   | 10.71429 |
| Rheumatoid arthritis         | 2   | 7.142857 |
| Diabetes Mellitus            | 2   | 7.142857 |
| Multiple Myeloma             | 2   | 7.142857 |
| Chronic lymphocytic leukemia | 1   | 3.571429 |
| Non-Hodgkin lymphoma         | 1   | 3.571429 |
| Hodgkin lymphoma             | 1   | 3.571429 |
| Carcinoma Lung               | 1   | 3.571429 |
| IBD - Crohn disease.         | 1   | 3.571429 |

**Table 3: Etiology of Thalassemia**

| Type                                       | No. | %    |
|--|-----|------|
| Thalassemia trait                          | 9   | 81.8 |
| Delta B thalassemia                        | 1   | 9.0  |
| Double heterozygote HBE and B- thalassemia | 1   | 9.0  |

**Table 4: Gender vs Diagnosis**

| Gender | IDA |      | DX<br>AOCD |      | Thalassemia |      |
|--------|-----|------|------------|------|-------------|------|
|        | No. | %    | No.        | %    | No.         | %    |
| Male   | 21  | 34.4 | 16         | 57.1 | 2           | 18.2 |
| Female | 40  | 65.6 | 12         | 42.9 | 9           | 81.8 |
| Total  | 61  | 100  | 28         | 100  | 11          | 100  |

$\chi^2=6.414^a$ ;  $p=0.040$

**Table 5: Hemogram**

|      | IDA<br>Mean±SD<br>N=61 | AOCD<br>Mean±SD<br>N=28 | Thalassemia<br>Mean±SD<br>N=11 | p-value |
|------|------------------------|-------------------------|--------------------------------|---------|
| HB   | 6.970±1.5966           | 7.800±1.1512            | 8.000±0.9571                   | 0.012   |
| TRBC | 3.0123±0.72770         | 3.8961±0.60399          | 4.8591±0.95264                 | <0.001  |
| PLT  | 3.2170±1.30404         | 2.5679±0.72982          | 2.1109±0.62266                 | 0.002   |

**Table 6: Hemoglobin Indices**

|     | IDA<br>Mean±SD<br>N=61 | AOCD<br>Mean±SD<br>N=28 | Thalassemia<br>Mean±SD<br>N=11 | p-value |
|-----|------------------------|-------------------------|--------------------------------|---------|
| MI  | 24.2115±7.25806        | 15.5786±2.49345         | 13.5073±3.30384                | <0.001  |
| RDW | 19.466±1.9141          | 15.650±1.3304           | 15.409±1.0222                  | <0.001  |

**Table 7: Outpatient Department (OPD) / In-Patient Department (IPD) vs Diagnosis**

| OPD/IPD | Diagnosis |      |      |      |             |      |
|---------|-----------|------|------|------|-------------|------|
|         | IDA       |      | AOCD |      | Thalassemia |      |
|         | No.       | %    | No.  | %    | No.         | %    |
| OPD     | 27        | 44.3 | 8    | 28.6 | 9           | 81.8 |
| IPD     | 34        | 55.7 | 20   | 71.4 | 2           | 18.2 |
| Total   | 61        | 100  | 28   | 100  | 11          | 100  |

$\chi^2=9.092^a$ ; p=0.011

Varanasi, 2 patients (18.1%) were from Azamgarh, 1 patient (9.1%) from each of Mau, bhadohi, Gazipur, Balia districts of Uttar Pradesh. In this study iron deficiency anemia was present in 34.4% in males and 65.6% in females, anemia of chronic disease was present in 57% in males and 42.9 % in females and thalassemia was present in 18.2 % males and 81.8% in females, with p-value=0.040 which was statistically significant (Table 4). In this study, we observed that the mean hemoglobin in iron deficiency anemia patients was 6.970±1.59, in AOCD patients 7.800±1.15 and in thalassemia patients it was 8.000±0.95 with the P-value of 0.012 which was statistically significant. The mean total red blood cell count in iron deficiency anemia patients was 3.0123±0.72, in AOCD patients was 3.8961±0.60 and in thalassemia patients 4.8591±0.95 with the P-value of <0.001 which was statistically significant. The mean platelet count in iron deficiency anemia patients was 3.2170±1.30, in AOCD patients was 2.5679±0.72 and in thalassemia patients 2.1109±0.6 with the P-value of 0.002 which was statistically significant (Table 5). In this study, we observed that the mean Mentzer index in iron deficiency anemia patients was 24.2115±7.25, in AOCD patients 15.5786±2.49 and in thalassemia patients it was 13.5073±3.30 with the P-value of <0.001 which was statistically significant. The mean total red cell distribution width in iron deficiency anemia patients was 19.466±1.9141, in AOCD patients was 15.650±1.3304 and in thalassemia patients 15.409±1.0222 with the P-value of <0.001 which was statistically significant (Table 6). In this study, the mean serum iron, in iron deficiency anemia group

---

---

was  $20.28 \pm 6.232$ , in Anemia chronic disease patients  $79.04 \pm 26.001$  and in thalassemia patients was  $61.18 \pm 14$ . with the P- value of  $<0.001$  which was statistically significant.

The mean total iron binding capacity (TIBC) in iron deficiency anemia patients was  $434.41 \pm 77.3$ , in AOCD patients was  $252.07 \pm 64.223$  and in thalassemia patients was  $275.64 \pm 53.9$  with the P value of  $<0.001$  which was statistically significant. The mean serum ferritin in iron deficiency anemia patients was  $7.259 \pm 2.9$ , in AOCD patients it was  $322.750 \pm 229.4$  and in thalassemia patients it was  $160.727 \pm 79.3$  with the P- value of  $<0.001$  which was statistically significant. In this study the mean percentage saturation in iron deficiency anemia group was  $5.3308 \pm 2.16$ , in AOCD patients  $26.6000 \pm 8.25$  and in thalassemia patients was  $23.2000 \pm 5.26$ . with the P- value of  $<0.001$  which was statistically significant. In this study out of total 61 patients of iron deficiency anemia, 44.3% patients were from OPD and 55.7 % were from IPD. Out of total 28 patients of anemia of chronic disease 28.6% were from OPD and 71.4% were from IPD and 81.8 % of thalassemia patients were from OPD and 18.2% were from IPD with the P- value = 0.011 which was statistically significant (Table 7).

## DISCUSSION

The pathogenesis is well-defined, and a systematic approach to arriving at a clear diagnosis of microcytic hypochromic anaemia has been established. Similar to our analysis, the most common causes of microcytic hypochromic anaemia in the majority of series were IDA and thalassemia trait [6]. Chronic illness anaemia is the second most common cause of anaemia after iron deficiency anaemia. In AOCD, the peripheral blood film is generally normocytic. The advanced condition causes red cells to appear microcytic and hypochromic. Other less frequent diagnoses that must be considered are including sideroblastic anemia, chronic lead poisoning, and Xlinked sideroblastic anemia [7]. In this study out of a total of 100 patients of microcytic hypochromic anemia, 61% patients had iron deficiency anemia, 28 % patients had anemia of chronic disease anemia and 11% patients had thalassemia.

Iron deficiency is the most frequent haematological disorder, and iron deficiency anaemia is the most common cause of anaemia worldwide [8]. Although blood loss is a major cause of iron deficiency anaemia, dietary iron insufficiency remains the most common cause of iron deficiency anaemia in developing countries [9]. Iron deficiency can occur as a result of an iron-deficient diet, such as that followed by dedicated vegans [10].

Comparable to this study Patel et al. selected 100 anaemic patients from Shree Krishna hospital in GUJARAT in 2009 after obtaining a complete history and clinical evaluation [11]. They discovered 40 patients with iron deficiency anaemia in their investigation. Females were more affected than males. There were two peaks in age groups of 21-30 years and 31-50 years, and the majority of patients (53%) were found to have moderate iron deficiency. Kaur & Kaur discovered that 98% of female respondents and 56% of male subjects were anaemic in a recent study done in the rural population of Patiala, one of Punjab's major cities [12]. It was also suggested that women's poor nutritional profiles are positively

---

---

associated with haemoglobin levels.

The distribution of iron deficiency anaemia (IDA) across age groups was investigated in this study. IDA predominates in the elderly 61-70 years (32.7%) followed by reproductive age 21-30 years (21.3%) followed by 18% of cases in the age group of 51-60 year.

This study found that female patients had a higher prevalence of microcytic hypochromic anaemia (39% were male and 61% were female), and females were more prevalent across all age categories. In this study, iron deficiency anaemia was found in more females (65.6%) than men (34.4%), chronic disease anaemia was found in 57% of males and 42.9% of females, and thalassemia was found in 18.2% of males and 81.8% of females.

The majority of studies have discovered that patients with iron deficiency anaemia typically have substantial gastrointestinal lesions, especially those of the upper gastrointestinal tract. Cook et al. discovered 40% of patients had upper gastrointestinal tract lesions, while Kepczyk et al. discovered 55% of patients had upper gastrointestinal tract lesions [13, 14].

Upper gastrointestinal lesions were seen in 21.3% (13 of 61 iron deficiency anaemia patients) of our study participants. Upper gastrointestinal bleeds were caused by antral gastritis in 13.7% of cases, a duodenal ulcer in 10.3%, gastroesophageal varices in 6.8% of cases, and sliding hiatus hernia with gastritis in 3.4% of cases.

The rate of lower gastrointestinal tract abnormality in iron deficiency anemia patients was 13.5-30%. In these studies, the most common lower gastrointestinal lesion was found to be hemorrhoid (28.7%) [15, 16].

In our study, hemorrhoids were the most prevalent lower gastrointestinal lesion detected in 85.7% of iron deficiency anaemia patients, which was slightly higher than in the previous study. Other lower gastrointestinal pathology includes inflammatory bowel disease-ulcerative colitis (4.7%), colonic diverticula (4.7%), and colonic cancer (4.7%). Menorrhagia was the major cause of iron deficiency anaemia in females of reproductive age [17].

In this study, we observed that in patients with iron deficiency anemia, a total of 11 female patients had menorrhagia (18%), out of these the most common cause was dysfunctional uterine bleeding in 6 patients (54.5%) followed by uterine fibroid in 2 patients (18.1%) and other causes include uterine polyp, hypothyroidism, and carcinoma cervix.

According to J.B.Sharma et al., amebiasis and giardiasis are common, and increased iron loss from hookworm infestations, schistosomiasis, chronic malaria, excessive sweating, and blood loss from the stomach due to hemorrhoids are also major causes of anaemia in pregnancy [18].

In our study 3 patients (16.6%) had hookworm infestation and 1 patient (5.5%) had *Ascaris lumbricoides* infestation.

All these studies closely correlate with our study where iron deficiency anemia is more common in females (66.5%) than in males (34.4%), in females, the common age group were reproductive and post



---

---

menopausal age group 51-60 years, while in the male the common age group was elderly. The 2nd most common cause of microcytic hypochromic anemia is anemia of chronic disease (28%). The anemia of chronic disease/inflammation was more common in hospitalized patients. Out of the total patients with anemia of chronic disease, 28.6% were from OPD and 71.4% were from IPD. ACD has been observed in a number of situations, including severe trauma, diabetes mellitus, and geriatric anaemia, in addition to infections, inflammation, and cancer [19]. Chronic disease anaemia is still underdiagnosed and undertreated [20].

A recent research of 191 consecutive hospitalised elderly adults with anaemia discovered that 70% of patients had anaemia or chronic illness. Chronic renal failure was seen in 16% of patients with chronic anaemia. 71% of patients with chronic anaemia had an acute infection, 12% had malignancy, and 16% had a chronic infection, such as a pressure ulcer or a chronic autoimmune inflammatory illness [21]. In our study we observed that out of a total of 28 AOCD patients the most common cause was an infection - Tuberculosis in 11 patients (39.2%) followed by chronic kidney disease in 3 patients (10.7%), followed by systemic lupus erythematosus in 3 patients (10.7%), next includes 2 patients from each of rheumatoid arthritis, multiple myeloma, diabetes mellitus, and other causes includes non-Hodgkin lymphoma, Hodgkin lymphoma, Chronic lymphocytic leukemia, carcinoma lung, and Crohn disease.

In the elderly, around 10322% of anaemia is thought to be attributable to inflammation, as circulating IL 6 levels rise with age, though there are numerous other causes of anaemia that become more common with age, including iron efficiency and other diseases [22].

Chronic illness anaemia has been classified according to age groups. Following distribution, it is clear that the majority of patients suffering from chronic anaemia are between the ages of 41 and 70.

Anemia is common in tuberculosis patients, and it may be more prevalent in individuals who are infected with both TB and HIV [23]. More over three-quarters (77%) of TB patients without HIV were anaemic in one Malawi research, while 88% of TB/HIV coinfecting patients were anaemic [24]. Dr. Sunanda Mondal et al. examined Microcytic Hypochromic Anemia and categorised 150 cases into three groups: Group-1 (iron deficiency anemia IDA) cases 90 (60%), Group-2 (anaemia on chronic disease-ACD) cases 31 (21%), and Group-3 thalassemia cases 29 (19%). Iron deficiency anaemia (IDA) was found to be more common (84%) in reproductive-age females (31-40 years) than in pre or postmenopausal women (41-50 yrs.). The bulk of ACD instances discovered in Group 2 were in the elderly, who were suffering from various types of chronic illness. These age groups are primarily above 50, with men outnumbering women (74%) [25].

The finding and distribution of iron deficiency and AOCD in our study closely correlate to the above study.

Thalassemia (11% of the cases) is the third cause of microcytic hypochromic anaemia. In the Indian subcontinent, thalassemia is a common hereditary illness. Because severe alpha-deletion mutations are less common in this region, alpha-thalassemia is not a major issue in India. The carrier rate for -

---

---

thalassemia ranges between 3 and 17%. In India, the percentage of thalassemia carriers ranges from 1 to 80 percent. However, it is less clinically relevant than  $\beta$ -thalassemia [26].

In our study, we observed that out of a total of 11 thalassemia patients most common were  $\beta$ thalassemia traits in 81.8 %, followed by 9% of each Delta B – thalassemia and double heterozygous HBE and B thalassemia. Of these patients 18.2 % were males and 81.8% were females. The difference in the sex distribution is might be due to different age groups. In our study, we included the adult population mostly.

### **The Limitations of Our Study**

1. The sample size was small.
2. There was no control in our study.
3. This is a hospital-based study at a tertiary care center from a limited geographical region, and most of the patients are from indoor ward, So It could not represent the whole population of India.
4. Children were not included in the study, so the exact prevalence of thalassemia could not be defined.

### **CONCLUSION**

Anemia is not an illness in and of itself, but rather a symptom of another, hence finding the underlying cause is significantly more important. This study was undertaken to analyse the aetiologies of microcytic hypochromic anaemia, and it found that iron deficiency anaemia (IDA) is the most common cause, followed by chronic illness anaemia and thalassemia. All patients with Microcytic hypochromic anaemia should have a complete evaluation, including a hemogram and a peripheral blood film. Before iron supplementation, a serum iron profile, bone marrow iron stain, and haemoglobin electrophoresis must be performed to confirm the aetiology. People suffering from chronic illnesses, which form a large group as a result of nutritional insufficiency and anaemia from chronic diseases, can be avoided to some extent by the ongoing and uninterrupted implementation of anti-tuberculosis programmes in third-world countries such as India. Carrier screening programmes have been helpful in raising awareness of thalassemia among the general public in thalassemia-prevalent developing countries.

Although precise data on thalassemia prevalence in our country is not accessible. We discovered a significant number of patients with thalassemia characteristics in this investigation. To lessen the burden of thalassemia, mass awareness, premarital counselling, and prenatal diagnostics should be implemented.

### **Funding Support**

The authors declare that they have no funding support for this study.

### **Conflict of Interest**

The authors declare that there is no conflict of interest.

---

---

## REFERENCES

- [1] C M Chaparro and P S Suchdev. *Anemia epidemiology, pathophysiology, and etiology in low-and middle-income countries. Annals of the new York Academy of Sciences*, 1450(1):15–31, 2019.
- [2] P Dasharatham and V S Reddy. *A study of etiological and clinical profile of patients with severe anemia in a tertiary care hospital. Int J Adv Med*, 5:1422–1429, 2018.
- [3] Ministry of Health and Family Welfare. *National Family Health Survey (NFHS 5) 2019-2021*, 2022. Government of India.
- [4] P R Dallman. *Diagnosis of anemia and iron deficiency: analytic and biological variations of laboratory tests. The American journal of clinical nutrition*, 39(6):937–941, 1984.
- [5] M Wiciński, G Liczner, K Cadelski, T Kolnierzak, M Nowaczewska, and B Malinowski. *Anemia of Chronic Diseases: Wider Diagnostics-Better Treatment? Nutrients*, 12(6):1784, 2020.
- [6] W O Uprichard and J Uprichard. *Investigating microcytic anaemia. Bmj*, 346:3154, 2013.
- [7] J F Matos, L Dusse, K B Borges, R L De Castro, W Coura-Vital, and M D G Carvalho. *A new index to discriminate between iron deficiency anemia and thalassemia trait. Revista brasileira de hematologia e hemoterapia*, 38:214–219, 2016.
- [8] S Majid, M Salih, R Wasaya, and W Jafri. *Predictors of gastrointestinal lesions on endoscopy in iron deficiency anemia without gastrointestinal symptoms. BMC gastroenterology*, 8(1):1–7, 2008.
- [9] A Zhu, M Kaneshiro, and J D Kaunitz. *Evaluation and treatment of iron deficiency anemia: a gastroenterological perspective. Digestive diseases and sciences*, 55(3):548–559, 2010.
- [10] M Alleyne, M K Horne, and J L Miller. *Individualized treatment for iron-deficiency anemia in adults. The American journal of medicine*, 121(11):943–948, 2008.
- [11] S Patel, M Shah, J Patel, and N Kumar. *Iron deficiency anaemia in moderate to severe anaemic patients. Gujarat Medical Journal*, 64, 2009.
- [12] L Raman, M K Menon, and P K Devi. *Anaemia in pregnancy. Postgraduate obstetrics and gynaecology. volume 128 of 1, pages 45–51, 1986. 3rd edition: p 55-62. Hyderabad: Orient Longmans. 008 Jul.*
- [13] S F Clark. *Iron deficiency anemia. Nutrition in clinical practice*, 23(2):128–141, 2008.
- [14] M T Kepczyk and C S C Kadakia. *Prospective evaluation of gastrointestinal tract in patients with iron-deficiency anemia. Digestive diseases and sciences*, 40(6):1283–1289, 1995.
- [15] S Serefhanoglu, Y Buyukasik, H Emmungil, N Sayinalp, I C Haznedaroglu, H Goker, and O I Ozcebe. *Identification of clinical and simple laboratory variables predicting responsive gastrointestinal lesions in patients with iron deficiency anemia. International journal of medical sciences*, 8(1):30, 2011.
- [16] D C Rockey. *Occult gastrointestinal bleeding. New England Journal of Medicine*, 341(1):38–46, 1999.
- [17] A Jacobs and E B Butler. *Menstrual blood-loss in iron-deficiency anaemia. Lancet*, 2:407–409,

---

---

1965.

[18] J B Sharma, B S Arora, and S Kumar. *Helminth and protozoan intestinal infections: An important cause for anemia in pregnant women in Delhi. J ObstetGynaecol Ind*, 51(6):58–61, 2000.

[19] E A Price and S L Schrier. *Unexplained aspects of anemia of inflammation. Advances in hematology*, 2010.

[20] G Weiss. *Pathogenesis and treatment of anaemia of chronic disease. Blood reviews*, 16(2):87–96, 2002.

[21] E Joosten and P Lioen. *Iron deficiency anemia and anemia of chronic disease in geriatric hospitalized patients: How frequent are comorbidities as an additional explanation for the anemia? Geriatrics and gerontology interna-*

22] B J Mccranor, J M Langdon, O D Prince, L K Femnou, A E Berger, C Cheadle, and C N Roy. *Investigation of the role of interleukin-6 and hepcidin antimicrobial peptide in the development of anemia with age. Haematologica*, 98(10):1633–1640, 2013.

[23] P Papathakis and E Piwoz. *Nutrition and Tuberculosis: A review of the literature and considerations for TB control programs. United States Agency for International Development, Africa's Health 2010 Project*, 1, 2008.

[24] M Van Lettow, C E West, J W M Van Der Meer, F T Wieringa, and R D Semba. *Low plasma selenium concentrations, high plasma human immunodeficiency virus load and high interleukin-6 concentrations are risk factors associated with anemia in adults presenting with pulmonary tuberculosis in Zomba district. European journal of clinical nutrition*, 59(4):526–532, 2005.

[25] Sunanda Mondal et al. *A Study on Microcytic Hypochromic Anaemia with the Help of Parameters: CBC with RBC Indices, Bio chemical Markers (Iron Profile) and HPLC - A Hospital Based Observational Study. JMSCR*, 05(07):24986–24992, 2017.

[26] D R Higgs, S L Thein, and W G Wood. *Distribution and population genetics of the thalassemias. 2001. In: Weatherall DJ, Clegg JB, editors. The Thalassemia Syndromes. 4th ed. Oxford: Blackwell Science, pp. 237–84. ISBN: 978-0-470-69594-4.*

---

---

# Development and Validation of an HPTLC Method for Qualitative and Quantitative Estimation of Quercetin in *Glinus oppositifolius* (L.)

Tushar Adhikari, Prerona Saha\*

Department of Pharmaceutical Chemistry, Guru Nanak Institute of Pharmaceutical Science and Technology, Panihati, Kolkata - 700114, West Bengal, India

## **ABSTRACT**

*Glinus oppositifolius* (L.) is a perennial herb used in Indian folk medicine as a stomachic, aperients, antiseptic, uterine stimulant, and to promote menses and lochia. The reported pharmacological activities of this plant are immunomodulatory, hepatoprotective, anthelmintic, anti-hyperglycemic etc. activities. To an HPTLC densitometric method was developed and validated for the qualitative and quantitative estimation of quercetin in *Glinus oppositifolius* (L.) available from West Bengal. The shade-dried leaves of *Glinus oppositifolius* (L.) were extracted with Methanol. HPTLC analysis was carried out on aluminum-backed silica gel 60 F254 plates with Ethyl acetate:Toluene-Formic acid 5:4:0.2 (v/v/v) as mobile phase. The HPTLC densitometric method was developed and validated as per ICH guidelines for estimation of quercetin. Total Flavonoid Content (TFC) is  $102.95 \pm 3.85$  mg QE/gm. In HPTLC analysis, *G. oppositifolius* ethanolic extract showed a maximum of 8 well-resolved peaks at  $R_f$  0.005, 0.098, 0.266, 0.466, 0.655, 0.724, 0.776 and 0.827. Well separated and compact spots ( $R_f$ ) of quercetin ( $0.81 \pm 0.06$ ) were detected. The regression equation obtained was  $y = 0.0002x + 0.0019$ , with a correlation coefficient ( $R^2$ ) of 0.9852. The linearity range ( $\mu\text{g/spot}$ ) 20-100. Quercetin content was found to be  $0.25 \pm 0.0047$  mg of quercetin/100gm sample. The developed method was found precise, robust and accurate and was successfully used for the detection and quantification of quercetin in *Glinus oppositifolius* (L.) and the quantities of quercetin was  $0.25 \pm 0.0047$  mg of quercetin/100gm sample.

**Keywords:** Quercetin, HPTLC, *Glinus oppositifolius* (L.), Flavonoid

## **INTRODUCTION**

Herbal medicines have been used to treat ailments since time immemorial. The fact that many contemporary medicines are derived from higher plants is evidence that plant-derived natural products play an important role in modern day drug discovery. A majority of recent research focuses on the phytochemical investigation of plants with ethnopharmacological evidence. India has one of the most ancient, diverse, and rich cultural traditions associated with the utilization of medicinal plants. Herbs, being easily available to humans, have been extensively researched for their medicinal properties. Some medicinal plants utilised in Ayurvedic formulations have been investigated thoroughly, while others remain unexplored [1]. One such less explored herb is *Glinus oppositifolius* (L.), commonly known as Indian carpetweed, which is freely available in West Bengal and its neighbouring regions, and is used as a vegetable.

*Glinus oppositifolius* (L.) August to December is a profusely branched, annual/ perennial herb, commonly found within the tropics in areas of low elevation. The plant is slender spreading, ascending or almost prostrate with stems up to 40 cm long [2]. The plant generally grows close to the ground in open

---

---

areas, lake shores and river banks. The leaves are usually arranged oppositely in an unequal whorl, in sets of 4-5 leaves. Each leaf is 0.5 to 1.5 cm in size. The shape of the leaves is mostly oblanceolate or linear lanceolate, but sometimes spatulate or rounded leaves are also seen – varying from one region to another. They are green in colour with a sub-acute or acute leaf apex. The leaves have an unpleasant odour and are bitter in taste [3, 4]. The root of *Glinus oppositifolius* (L.) is a typical taproot.

There is a primary and secondary root system for the tap. There are a number of rootlets, each varying from 0.1 to 0.4 cm thick [4]. Flowers are white and arranged in cluster form in axillary fashion. Around 3 to 6 flowers are attached with node [3]. Ethnomedicinal Uses of *Glinus oppositifolius* *Glinus oppositifolius* (L.) is used by several different communities as ethnomedicine, like in Taiwan, Mali, Bangladesh and mostly the southern parts of India. In addition to its portions (usually leaves) being eaten as vegetables, it is useful as an anti-diabetic medication. The plant also has some nutritional benefit because it is commonly used as a dietary staple, particularly in South India.

In the Salem district of Tamil Nadu, India, folk healers treat poisonous animal bites using the leaves of the *Glinus oppositifolius* (L.) plant [5]. The tribes of Maharashtra's Nandurbar district utilise the whole plant extract as a carminative, stomachic, and tonic [6]. According to the Narikorava tribe of Tamil Nadu, one of the significant applications for this herb is as a tonic for new mothers to alleviate postpartum weakness [7]. For liver diseases, it can be used as a bitter tonic [8]. In Maldah district of West Bengal, the root paste of this plant is given orally to treat dysentery [9].

In traditional Mali (West Africa) medicine, dried stems and leaves are ground into a fine powder, mixed with food, and used to alleviate gastrointestinal pain and jaundice [10]. In Thailand, the whole plant aqueous extract of *Glinus oppositifolius* (L.) has been traditionally used as expectorant and antipyretic [11]. In Bangladesh, *Glinus oppositifolius* (L.) extracts have long been traditionally used for the treatment of inflammation, joint pain, fever, diarrhoea, and skin disorders [12]. Whole plants are used in Bangladesh's southern district Noakhali to treat earaches, skin conditions, gastritis, and appetite loss [13]. According to folklore in Philippines, the plant has anti-diabetic and antimicrobial effects [14]. There have been reports of a variety of phytochemical compounds from *G. oppositifolius* (L.) in recent years, but there hasn't yet been a thorough investigation using a purified chemical compound from the plant. Aim of the present study is to HPTLC densitometric method was developed and validated for the qualitative and quantitative estimation of quercetin in *Glinus oppositifolius* (L.) available from West Bengal.

## **MATERIALS AND METHODS**

### **Collection of Plant Material**

The whole plant of *Glinus oppositifolius* (L.), locally known as 'Gima shaak', was procured from a local market in Kolkata, By the Central National Herbarium (CNH), Botanical Survey of India, Shibpur, West

---

---

Bengal, the plant was identified.

### **Chemicals**

Standard quercetin was obtained from Loba Chemie Pvt. Ltd. All chemicals and reagents used for preliminary phytochemical analysis were of analytical grade. The solvents used were all of HPLC standard

### **Preparations of Plant Extract for Detection and Quantification of Quercetin in Methanolic Extract of *Glinus oppositifolius* (L.)**

The leaves of *Glinus oppositifolius* (L.) were air dried, coarsely ground up, and then extracted thoroughly by macerating with methanol for seven days. Using a rotary vacuum evaporator, the solvent was evaporated to dryness under decreased pressure, and then each of the leftovers was individually dissolved in methanol in 50 ml volumetric flasks.

### **Preliminary Phytochemical Analysis**

The plant extracts of *Glinus oppositifolius* (L.) were assessed qualitatively for their phytochemical content using standard methods [15–17]. The extracts were tested for the presence of flavonoids, glycosides, alkaloids, terpenoids, tannins, phenols and saponins (Table 1).

### **Determination of Total Flavonoid Content**

Total flavonoid content of methanolic extract of *Glinus oppositifolius* (L.) was determined by aluminum chloride colorimetric method. The reaction mixture contained 1 ml of solution of extracts in the concentration of 1 mg/ml and 1 ml of 2% aluminum chloride solution dissolved in water. At room temperature, the sample was incubated for one hour. At 415 nm, the absorbance was measured. The same procedure was repeated for the solution of quercetin (standard) and the calibration line was constructed.

Based on the measured absorbance, the calibration line; then the content of flavonoids in the extract was expressed in terms of quercetin equivalent.

### **Solvent Selection**

The development of an appropriate TLC method for the measurement of quercetin in the methanolic extract of *G. oppositifolius* involved screening a number of different solvent systems. For these goals, movable phases were tested:

Toluene: Ethyl acetate: Formic acid (5:4:0.2v/v/v)

Ethyl acetate: Toluene: Formic acid (5:4:0.2v/v/v)

### **HPTLC Fingerprinting**

HPTLC studies were carried out following the method of Adhikari et al. [18].

---

---

### **Sample Preparation**

The standard and the methanolic extract were dissolved in 1ml of chromatographic grade methanol, which is used for sample application on HPTLC plate's pre-coated silica gel 60F 254 aluminum sheets.

### **Developing Solvent System**

A number of solvent systems were tried for extract, but the satisfactory resolution was obtained in the solvent Ethyl acetate: Toluene: Formic acid (5:4:0.2 v/v/v).

### **Sample Application**

Samples were applied on pre-coated silica gel 60F 254 aluminum sheets with the help of Linomat 5 applicator attached to CAMAG mark HPTLC system.

### **Development of Spots**

After the application of sample, the chromatogram was developed in Twin trough glass chamber 10\*10 cm saturated with the solvent Ethyl acetate:

Toluene: Formic acid (5:4:0.2 v/v/v) for 20 min.

### **Detection of Spots**

The air-dried plates were viewed in white light, UV  $\lambda$  254nm and UV  $\lambda$  366nm with and without staining with 10% H<sub>2</sub>SO<sub>4</sub> solution. The chromatogram was scanned by Densitometry TLC Scanner 4. The R<sub>f</sub> value and fingerprint data were recorded.

### **Method Validation**

Validation studies ensure the suitability and reproducibility of the method in analyzing the desired analyte. The method was validated for linearity, Limit of Detection (LOD), Limit of Quantification (LOQ), specificity and precision (repeatability) as per the ICH guidelines [19].

### **Linearity**

Dilutions of standard in the range of 20-100 ng per band were analyzed in triplicate to prepare five-point linear calibrations. The plates were created, scanned, and given a quantitative assessment. Peak area and concentration were plotted to produce calibration curves. By averaging the results of the regression analysis performed on these plots, linearity was established.



---

---

## Precision

Two levels of precision were assessed in accordance with ICH recommendations. Repeatability was determined as intraday precision whereas intermediate precision was determined by carrying out interday variation for the determination of quercetin levels of 20, 40, 60, 80 and 100 ng per band in triplicates.

## Robustness

The suggested TLC densitometric method's robustness was assessed in order to assess the impact of tiny, intentional alterations to the chromatographic conditions during the detection of quercetin. The polarity of the mobile phase was changed to assess robustness.

## LOD and LOQ

The values for the signal-to-noise ratios for the limits of detection (LOD) and quantification (LOQ) were found to be 3:1 and 10:1, respectively.

## Specificity

The specificity of the method was ascertained by analyzing the standard quercetin and extract. By contrasting the R<sub>f</sub> values and spectra of the spot with those of the standard, the presence of quercetin in the spot in the sample was verified. By comparing the spectra at three different levels, namely the peak start, peak apex, and peak end positions of the spot, the peak purity of quercetin was determined.

## RESULTS

### Phytochemicals Screening

Table 1 displays all of the phytochemical analysis' findings. In the study tannins, glycosides, flavonoids and terpenes were determined in methanolic extract of *Glinus oppositifolius* (L.).

### Total Flavonoid Contents

Five concentrations of standard Quercetin (20 µg/ml to 100 µg/ml) were used to prepare the standard

**Table 1: Phytochemical Analysis**

| Secondary metabolite | Phytochemical Test    | Ethanol Extract |
|----------------------|-----------------------|-----------------|
| Alkaloid             | Dragendorff's Test    | -               |
|                      | Hager's Test          | +               |
| Glycoside            | Salkowski test        | +               |
|                      | Liebermann test       | +               |
|                      | Keller- Kilani test   | +               |
|                      | Alkaline reagent test | +               |
| Flavonoid            | Shinoda test          | +               |
|                      | Lead acetate test     | -               |
| Tannin               | Ferric Chloride test  | +               |
|                      | Chloroform test       | +               |
| Terpenoid            | Frothing Test         | +               |

**Table 2: Linear Regression Data for the Calibration Curve of Quercetin**

| Linear Regression Parameter                   | Data                   |
|---|------------------------|
| Linearity range ( $\mu\text{g}/\text{spot}$ ) | 20-100                 |
| Regression equation                           | $y = 0.0002x + 0.0019$ |
| Correlation coefficient                       | 0.9852                 |
| Slope   | 0.00019005             |
| Intercept                                     | 0.001859               |
| SE of intercept                               | 0.00089                |
| SD of intercept                               | 0.00199                |

**Table 3: Recovery Study for Proposed Method (n=3)**

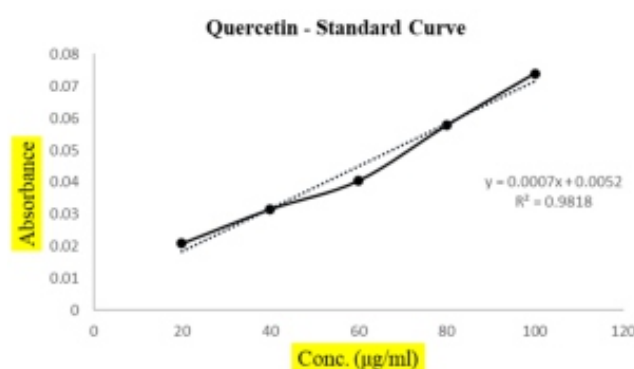
| Excess drug added to analyte (%) | Concentration found ( $\mu\text{g}\pm\text{SD}$ ) | % recovery | %RSD |
|----------------------------------|---|------------|------|
| 50                               | 50.37 $\pm$ 0.03                                  | 100.75     | 0.06 |
| 100                              | 91.29 $\pm$ 1.8                                   | 91.29      | 1.97 |
| 150                              | 154.59 $\pm$ 1.89                                 | 103.06     | 1.22 |

**Table 4: Precision of the Proposed Method (n=3)**

| Conc. ( $\mu\text{g}/\text{ml}$ ) | Repeatability (Intra-day precision) |            |      | Repeatability (Intra-day precision) |            |      |
|-----------------------------------|-------------------------------------|------------|------|-------------------------------------|------------|------|
|                                   | Area $\pm$ SD                       | Std. error | %RSD | Area $\pm$ SD                       | Std. error | %RSD |
| 100                               | 0.025 $\pm$ 0.00025                 | 0.00014    | 0.98 | 0.037 $\pm$ 0.00034                 | 0.0002     | 0.92 |
| 100                               | 0.021 $\pm$ 0.00028                 | 0.00016    | 1.33 | 0.038 $\pm$ 0.00034                 | 0.0002     | 0.88 |
| 100                               | 0.024 $\pm$ 0.00032                 | 0.00018    | 1.31 | 0.039 $\pm$ 0.00040                 | 0.00023    | 1.01 |

**Table 5: Robustness of the Propose HPTLC Method (n=3)**

| Con ( $\mu\text{g}/\text{ml}$ ) | Original Mobile Phase | Used Mobile Phase |      | Area $\pm$ SD         | %RSD | $R_f$ |
|---------------------------------|-----------------------|-------------------|------|-----------------------|------|-------|
| 100                             | 5:4:0.2               | 5:4:0.3           | +0.1 | 0.03727 $\pm$ 0.00048 | 1.30 | 0.85  |
|                                 |                       | 5:4:0.2           | 0    | 0.03916 $\pm$ 0.0028  | 0.90 | 0.81  |
|                                 |                       | 5:4:0.1           | -0.1 | 0.06089 $\pm$ 0.00066 | 1.08 | 0.82  |

**Figure 1: Standard Curve of Quercetin**

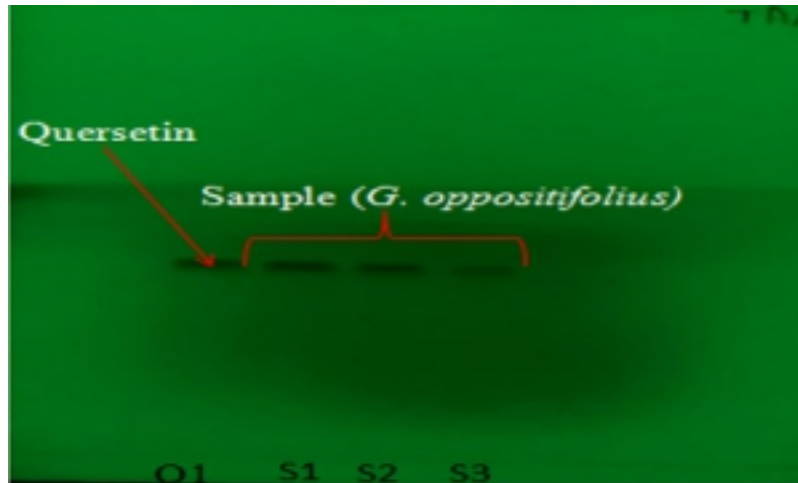


Figure 2: HPTLC Plate Showing Bands of Standard Quercetin (Q1) and Sample (S1-S3) at 254nm

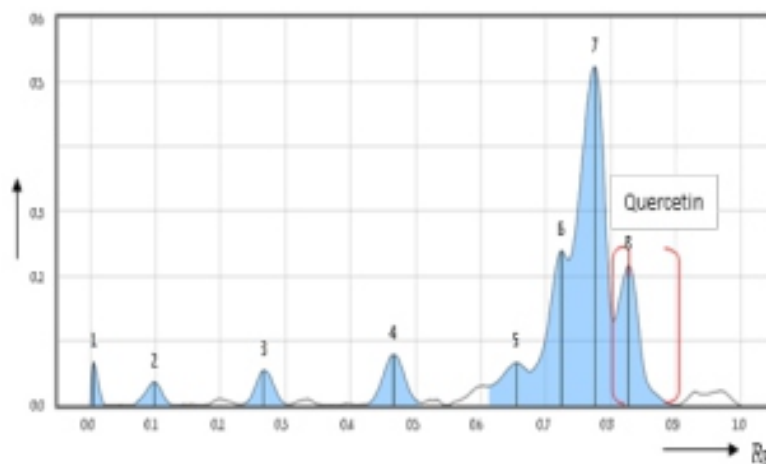


Figure 3: HPTLC Chromatogram of Glinus oppositifolius (L.)

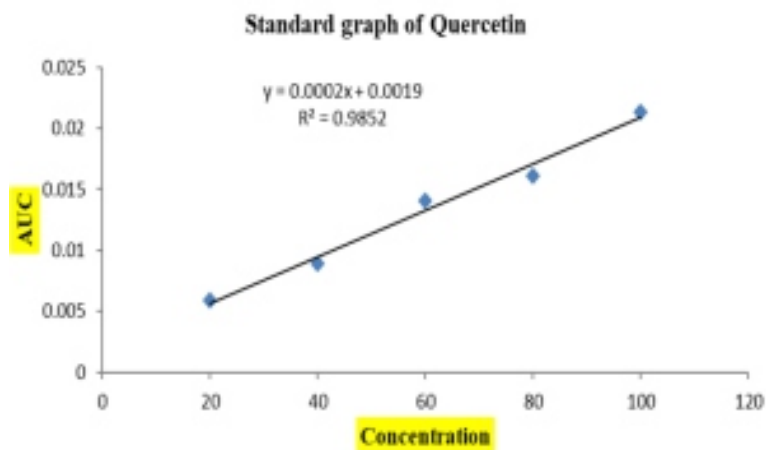
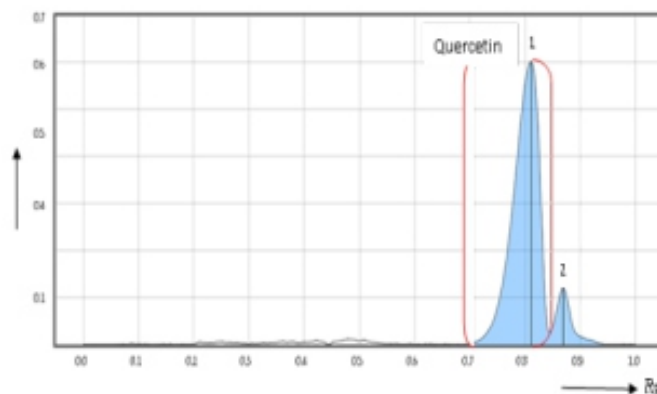


Figure 4: Regression Curve of Standard Quercetin



**Figure 5: HPTLC Chromatogram of Standard Quercetin**

curve -  $y = 0.0007x + 0.0052$ ;  $R^2 = 0.9818$  (Figure 1) used for the determination of total flavonoid content in the sample extracts, as shown in the below.

Total flavonoid content represented as Quercetin equivalent (QE) per gram of sample was tested in the methanol extract. The absorbance for each extract was measured in triplicate and results were calculated as their mean. Total flavonoid content in the methanol extract of *Glinus oppositifolius* (L.)  $102.95 \pm 3.85$  mg QE/ gm.

### Solvent Selection

A clear, compact, and well-resolved band for quercetin was obtained via ascending development using ethyl acetate-toluene-formic acid (5:4:0.2v/v/v). This band's  $R_f$  value was  $0.81 \pm 0.06$ . Figure 2 shows band of standard quercetin (Q1) and different volume of sample solution (S1-S3) at 254nm.

### HPTLC Fingerprinting

The results of the HPTLC fingerprinting of methanolextract of *Glinus oppositifolius* (L.) at 254 and 366nm are given in Figure 3. The methanol extract showed a maximum of 8 well resolved peaks, at  $2\mu\text{L}$  sample volume, with  $R_f$  values of 0.005, 0.098, 0.266, 0.466, 0.655, 0.724, 0.776 and 0.827.

Among these peaks, the peak at  $R_f$  value 0.827 showed the highest peak area of 16.22%. The peak corresponding to  $R_f$  value 0.827 showed a sharp peak and significant area of 16.22%, was identified as quercetin.

### Method Validation

According to the calibration plot in Figure 4, the response is a linear function of quercetin concentrations between 20-100 $\mu\text{g/ml}$ .

---

---

The slope, intercept, and correlation coefficient were 0.00019, 0.001859 and 0.9852 respectively. Table 2 displays the linear regression information for the quercetin calibration curve.

### **Recovery Study**

Results from recovery studies, which are listed in Table 3, showed good accuracy and fell within acceptable ranges (91.29 to 103.06%).

### **Precision**

Table 4 displays the findings from the determination of repeatability and intermediate precision, expressed as SD (%). For repeatability, RSD fell between 0.98 and 1.33, and for intermediate precision, it fell between 0.88 and 1.01. These small values demonstrated the method's accuracy.

### **Robustness**

Results of robustness are shown in Table 5. Low values of %RSD (0.09- 1.30) were obtained after introducing small deliberate change into the densitometric TLC procedure proved the robustness of the proposed HPTLC method.

### **Limit of Detection and Limit of Quantification**

The suggested approach's LOD and LOQ for quercetin were determined to be 34.62 and 104.91 µg/spot, respectively, demonstrating that the method may be utilised successfully for quercetin detection and quantification in a range of conditions.

### **Method Development**

The mobile phase composition was optimised with the goal of creating a reliable and accurate densitometric HPTLC technique for the measurement of quercetin. The mobile phase Ethyl acetate-Toluene Formic acid 5:4:0.2 (%v/v/v) exhibited a crisp, symmetrical, and well-resolved peak at R<sub>f</sub> value of (0.81±0.06) (Figure 5).

### **Quantification of Quercetin in the Methanolic Extract of *Glinus oppositifolius* (L.)**

By contrasting the single spot at R<sub>f</sub> = 0.81±0.06 (Figure 5) of the quercetin peaks from the methanolic extracts of the leafy vegetable *Glinus oppositifolius*(L.) with those obtained by chromatography of the standard under the same circumstances. Using the standard concentration and AUC, the quercetin content in methanolic extracts of *Glinus oppositifolius* (L.) is 0.258± 0.0047 mg of quercetin /100g sample.

---

---

## DISCUSSION

Plant medicines have been used to treat illnesses for as long a time in the history of mankind. Many contemporary medications have their origins in higher plants. Ayurveda, the traditional medical system of India, has made a variety of therapeutic claims regarding these plant-based medicines. However, it is crucial to support the varied medical benefits of the herbs with scientific evidence.

For a variety of reasons, the stage of ignorance for plant medicine is fast changing. First, issues with side effects of contemporary medications have rekindled interest in plants as a significant source of novel drug candidates. Second, since the majority of the already known lead structures have already been used, pharmaceutical scientists are in search for newer lead compounds from plants [20]. Traditional wisdom of the indigenous people can provide new sources for discovering leads. Third, herbal remedies have achieved remarkable success in the recent years.

The present study was undertaken to prepare the HPTLC Fingerprint profile of the plant *Glinus oppositifolius*(L.) (also known as Gima shaak) for the identification of compounds present in its extracts, as well as to quantify the identified flavonoid from it. Literature survey was conducted to find out the ethnomedicinal uses of the plant in several tribes of India, as well as in other countries like Taiwan, Mali and Bangladesh.

The methanol crude extract of *G. oppositifolius* (L.) was used for the identification of the plant secondary metabolites or phytochemicals present by the standard phytochemical screening tests. The methanol extract tested positive for most of the phytochemical tests, indicating presence of alkaloids, glycosides, flavonoids, terpenoids, tannins and saponins (Table 1).

The total flavonoid content of the plant extracts was estimated using the Aluminium chloride method, using quercetin as the standard. The principle behind this assay procedure is that aluminium chloride forms acid-stable complexes with the C-4 keto groups and either the C-3 or C-5 hydroxyl groups of flavones and flavonols present in the sample. Additionally, it combines with the ortho-dihydroxyl groups on the A or B ring of flavonoids to produce complexes that are acid labile [21]. The concentration of flavonoids present in the reaction media linearly affects the intensity of the light absorbed, thus useful in estimating the flavonoid content in the sample. In this study, higher amount of TFC was obtained in the ethanolic extract ( $102.95 \pm 3.85$  mg QE/ gm sample).

Following development, 10% H<sub>2</sub>SO<sub>4</sub> solution spraying reagents are applied to the TLC plates. After being sprayed with a 10% H<sub>2</sub>SO<sub>4</sub> solution, quercetin turned up as a red colour spot in both the sample

---

---

and the reference. Under chromatographic conditions, the R<sub>f</sub> value of quercetin extracted from *Glinus oppositifolius* (L.) was almost identical to that of the reference standard. One of the solvent systems was discovered to be suitable for running the sample after all 2 were analyzed. Therefore the Ethyl acetate: Toluene: Formic acid (5: 4: 0.2 v/v/v) can be considered as good solvent system (Figure 3). High Performance Thin Layer Chromatography (HPTLC) is a very useful technique for the analytical validation of novel natural product forms. HPTLC is currently becoming one of the best methods for ensuring product quality, purity, stability, as well as for identification, or, validation of an herbal product's complex composition. In this study, HPTLC was used to develop the chromatographic fingerprint profile of the methanolic extract of *Glinus oppositifolius* (L.) in the optimized mobile phase Ethyl acetate: Toluene: Formic acid (5: 4: 0.2 v/v/v). The pattern of the fingerprint profile obtained from this study can be used for the quality control of the plant sample. The identified compound from the chromatogram of this plant is Quercetin, having R<sub>f</sub> value 0.82. Quantification of quercetin was also carried out to estimate the amount of quercetin content per gram of plant sample. Quercetin content was found to be  $0.258 \pm 0.0047$  mg of quercetin /100gm sample.

## CONCLUSION

The presence of flavonoids in the methanolic extract of the plant could be responsible for its anti-inflammatory, anti-viral and immunomodulatory activity. HPTLC Fingerprint profile of the methanolic extract was obtained, which could be used for authentication and quality control of the herbal plant or other herbal formulations containing this plant. The flavonoid identified from the plant is quercetin, at R<sub>f</sub> value 0.82, which is being reported for the first time from this plant *Glinus oppositifolius* (L.). The flavonoid was quantified by comparing the area under the curve with standard quercetin and the quantity of quercetin is  $0.258 \pm 0.0047$  mg of quercetin /100g sample.

## Funding Support

The authors declare that they have no funding support for this study.

## Conflict of Interest

The authors declare that there is no conflict of interest.

## REFERENCES

[1] N Hari and V P Nair. Preliminary Phytochemical Evaluation and HPTLC Fingerprint Profile of *Jasminum azoricum* L. *Int J Sci Res Sci Eng*

- [2] C Y Ragasa, D L Espineli, E H Mandia, M J Don, and C C Shen. A new triterpene from *Glinus oppositifolius*. *Chinese Journal of Natural Medicines*, 10(4):284–286, 2012.
- [3] S T Ramaseshan, P Pitchaiah, V Bharti, K K Ramakrishna, V Gaddam, D Tewari, and D K Singh. Pharmacognostical, Phytochemical and Nutritional Evaluation of *Glinus oppositifolius* (L.) Aug. DC. *Pharmacognosy Journal*, 8(1), 2016.
- [4] R K Dewangan, S Dubey, and A K Dixit. Pharmacognostical and Qualitative Phytochemical Study of *Glinus oppositifolius* (Linn.) Aug. DC An Important Ethnobotanical Plant. *GIS Sci J*, 8:2105–2119, 2021.
- [5] T Thirunarayanan. Ethnobotanical survey on Folk Medicine in the management of animal bite poisons in the forest tract of Salem region of Tamil Nadu, India. *International Journal of Pharmacology and Clinical Sciences*, 2(2), 2013.
- [6] N Dongarwar, Uma Thakur, and S Dongarwar. Ethnomedicines Among Some Tribes Of Nandurbar District Of Maharashtra (India). *Life Sci LeaŶl*, 4:48–53, 2012.
- [7] G Siromoney, L D Giles, and C Livingstone. Herbal medicines of the Narikoravas. *Folklore*, 14(10):363–369, 1973.
- [8] C P Khare. *Indian medicinal plants: an illustrated dictionary*. 2008. Springer Science and Business Media.
- [9] M Chowdhury and A P Das. Inventory of some ethno-medicinal plants in wetlands areas in Maldah district of West Bengal. *Pleione*, 3(1):83–88, 2009.
- [10] K T Inngjerdingen, S C Debes, M Inngjerdingen, S Hokputsa, S E Harding, B Rolstad, and B S Paulsen. Bioactive pectic polysaccharides from *Glinus oppositifolius* (L.) Aug. DC., a Malian medicinal plant, isolation and partial characterization. *Journal of ethnopharmacology*, 101(1-3):204–214, 2005.
- [11] P Sahakitpichan, W Disadee, S Ruchirawat, and T Kanchanapoom. L-(–)-(N-trans Cinnamoyl)-arginine, an Acylamino Acid from *Glinus oppositifolius* (L.) Aug. DC. *Molecules*, 15(9):6186–6192, 2010.
- [12] N Hoque, M Z Imam, S Akter, M E H Mazumder, S R Hasan, J Ahmed, and M S Rana. Antioxidant and antihyperglycemic activities of methanolic extract of *Glinus oppositifolius* leaves. *Journal of Applied Pharmaceutical Science*, pages 50–53, 2011.
- [13] R Bhowmik, M R Saha, M A Rahman, and M A U Islam. Ethnomedicinal survey of plants in the Southern District Noakhali. *Bangladesh Pharmaceutical Journal*, 17(2):205–214, 2014.
- [14] C Y Ragasa, E C Cabrera, O B Torres, A I Buluran, D L Espineli, D D Raga, and C C Shen. Chemical constituents and bioactivities of *Glinus oppositifolius*. *Pharmacognosy Research*, 7(2):138, 2015.
- [15] O O Odebiyi and E A Sofowora. Phytochemical screening of Nigerian medicinal plants II. *Lloydia*, 41(3):234–246, 1978.



- 
- 
- [16] G E Trease and W C Evans. *Phenols and phenolic glycosides*. In *Textbook of Pharmacognosy*, volume 12, pages 343–383, 1989. Tindall and Co Publishers, London, UK.
- [17] B N Shah and A K Seth. *Textbook of Pharmacognosy and Phytochemistry*. 2010.
- [18] T Adhikari and P Saha. *Quantitative Estimation of Immunomodulatory Flavonoid Quercetin by HPTLC in Different Leafy Vegetables Available in West Bengal*. *Pharmacognosy Research*, 14(4), 2022.
- [19] R C Guy. *International Conference on Harmonisation. Encycl Toxicol Third Ed*, 2:1070–1072, 2014.
- [20] B Patwardhan. *Ayurveda: The designer medicine*. *Indian drugs*, 37(5):213–227, 2000.
- [21] G C Bag, P G Devi, and T H Bhaigyabati. *Assessment of total flavonoid content and antioxidant activity of methanolic rhizome extract of three Hedychium species of Manipur valley*. *International Journal of Pharmaceutical Sciences Review and Research*, 30(1):154–159, 2015

---

---

# Madhuca longifolia leaf extract mediated synthesis of ZnO nanoparticles and their Antibacterial, Antioxidant, and Photocatalytic activity

Rajani\*1 , Rishi Kesh Meena2, Preeti Mishra2

1Government PG College, Kekri, Ajmer, Rajasthan, India

2Department of Botany, University of Rajasthan, Jaipur, Rajasthan, India

## ABSTRACT

*The biogenic synthesis of ZnO NPs is a promising substitute for the standard method of NP synthesis. In the current study, ZnO nanoparticles were produced biologically. Leaf extract from the Madhuca longifolia (M-ZnO Nps) plant was used to create ZnO NPs, which were then examined using UV-vis, XRD, FTIR, SEM, and TEM. SEM and TEM examination and XRD validated the size and crystalline nature of Zinc oxide nanoparticles, respectively. Functional groups involved in the production of ZnO NPs were visible in the FTIR spectra. By scavenging DPPH free radicals at various concentrations, the antioxidant activity of green ZnO NPs was determined. By using the agar well diffusion method, ZnO NPs were tested for their bactericidal potential against Gram-negative bacteria E. coli and Gram-positive bacteria Staphylococcus aureus bacterial strains. A 96% photodegradation of MB dye and 91% degradation of textile wastewater was observed in green-produced ZnO NPs when exposed to sunshine. The recent work proved that ZnO NPs have substantial antioxidant, antibacterial, and photocatalytic activity. Therefore, the study offers a straightforward, practical, economical, and ecologically secure green synthesis technique for the biofabrication of multifunctional ZnO nanoparticles.*

**Keywords:** Antibacterial activity, Antioxidant activity, Green synthesis, Madhuca longifolia, Photocatalytic activity, ZnO nanoparticles

## INTRODUCTION

Nanotechnology is a rapidly growing and widely accepted research field in modern material science with the purpose of synthesis of new materials at the nanoscale level. Many researchers reported that nanomaterials have various functions and huge efficiency that are not noticed in their bulk phase and nano-dimension particles are extensively studied due to having electronic, magnetic, catalytic, optical, antimicrobial, wound healing, and anti-inflammatory properties [1].

Zinc oxide is a well-known semiconductor (n-type) with low-coat, nontoxic, and photocatalytic properties. ZnO has a wide bandgap semiconductor with 3.2 eV and photocatalytic activity is a commonly investigated function of semiconductors [1]. Zinc oxide nanoparticles are well known for their wide range of applications in diverse fields. Due to the extremely low toxicity of ZnO nanoparticles, recent research works have paid high attention to their function and employment, especially in the biomedical field property. The demand and production of green ZnO NPs increased gradually because a better eco-

---

---

friendly alternative is required to avoid the use of high-energy inputs and toxic chemicals.

Looking at the harmful and toxic effects of nanomaterials on the environment, current research focused on a low-toxic, cost-effective, and ecofriendly green approach. The biological process of NPs synthesis using plant extracts, microorganisms, algae, and enzymes is considered a healthier substitute for existing processes of NPs synthesis because of their hazards to the environment [2, 3].

Nanotechnology has offered a ray of hope in the biomedical field as an antimicrobial and drug delivery agent for various diseases. However, the mechanisms of the bactericidal potential of ZnO NPs are still unknown, but Rajani et al.(2022) [4]; explain some mechanisms such as membrane disruption, generation of reactive oxygen species (ROS), disruption of the cell wall, leakage of nuclear and cytoplasmic material by the action of nanomaterials.

Textile wastewater contains a huge amount of non biodegradable hazardous dyes which causes some serious health and environmental issues. It is an immediate need to introduce a promising technology for dye removal with high efficiency and low toxicity. Nanotechnology has emerged as one of the prime technology with great potential for the degradation of textile dyes from wastewater more efficiently and effectively than previous methods. Current methods involve in the treatment of wastewater and water purification, are disgraced due to their insufficiency in water purification and high cost demands. Nanotechnology can help to conquer this issue by removing organic dyes, heavy metal pollutants, pesticides, and other chemical pollutants from water that are related to a serious hazard to the ecosystem because of their toxicity to water inhabitants and every living organism, including humans [5].

ZnO NPs are semiconductors that have photocatalytic properties so ZnO NPs can photodegrade textile dyes efficiently. ZnO NPs are widely employed as photocatalysts in the photodegradation of organic pollutants in air and water [6]. Vasantharaj et al. (2021) [7]; was successfully reported the degradation of synthetic textile dyes by green synthesized ZnO NPs using *Ruellia tuberosa* plant extract.

In this study, *Madhuca longifolia* plant leaf extract was applied for the facile green synthesis of ZnO nanoparticles. The phytochemistry study of *M. longifolia* plant shows that it is rich in protein, sugar, alkaloids, vitamin, phenolic compounds, saponins, triterpenoids, steroids, saponins, flavonoids, glycosides, etc. [8, 9]. ZnO nanoparticle synthesis using *M. longifolia* leaf extract is an environmentally benign synthetic method. *M. longifolia* has higher constituents of phenolic compounds which are amenable to the ZnO NPs synthesis.

These bio-compounds have reducing properties and acted as capping agents in the nanoparticle synthesis process. The bio-synthesized M-ZnO NPs were investigated for their antioxidant, antibacterial, and photocatalytic activities. The photodegradation performances of methylene blue (MB) dye by the green synthesized ZnO nanoparticles under sunlight irradiation were investigated.

## EXPERIMENTS

---

---

## Materials and Methods

Leaves of *Madhuca longifolia* were taken from the local garden of Jaipur, India. Plant leaves were cleaned with distilled water and dry to grind to make their powder. 5 g of *M. longifolia* plant leaves powder boiled in 100 ml distilled water for 20 minutes. After cooling, leaf extract was filtered using Whatman's filter paper and stored in the refrigerator for further use. Zinc nitrate hexahydrate ( $Zn(NO_3)_2 \cdot 6H_2O$ ) was used for ZnO NPs synthesis. MB dye was purchased from Thermo Fisher Scientific company, India. Textile dye samples were collected from the textile industry area, Sanganer, Jaipur.

## Biosynthesis of ZnO Nps

8 gm zinc nitrate was added into 25 ml distilled water and heated at 60°C. 50 ml *M. longifolia* plant leaf extract was added drop by drop into the heated zinc nitrate solution under the continuous stirrer. The solution was continuously stirred until a pale yellow colour paste was obtained. The paste was dried in the furnace at 400°C for 2 hours. The ZnO NPs were collected and stored for further characterization and applications.

## Characterization

The bio-synthesized ZnO NPs were sonicated before characterization and every application for uniform dispersion and obtaining higher efficiency. The ZnO NPs synthesis was confirmed by the UV-Vis spectroscopy of the compounds. The UV-Vis absorption peak of ZnO NPs centred at 376 nm. The optical analysis was carried out by the UV-Vis spectrophotometer (GENESIS 180). The morphology and size of ZnO NPs were analyzed by SEM images (Model ZESIS), at a working distance of 10 mm and a voltage of 20 kV. Transmission electron microscopy was performed using a TALOS HR-TEM apparatus operating at 80 kV. The crystalline structure and grain size were confirmed by XRD using Rigaku (Model SMART LAB) diffractometer. The functional groups and chemical composition of ZnO NPs were studied by using an FTIR spectrometer (Bruker ALPHA).

## Antioxidant activity

The free radical scavenging capacity of green synthesized ZnO NPs was evaluated against DPPH radical. DPPH (2,2-diphenyl-1-picryl-hydrazyl-hydrate) provides an easy method of determining antioxidant activity. DPPH was offered as a free radical source and ZnO NPs were applied as a radical scavenger. In the presence of ZnO NPs, the DPPH solution's deep violet colour gradually turns pale yellow. The absorbance at 517 nm gradually decreases as ZnO NP concentration increases. The ZnO nanoparticles' ability to scavenge free radicals is assessed by the reduced absorbance in the DPPH solution. M-ZnO NPs were treated in ten different doses to test the antioxidant potential of ZnO

---

---

nanoparticles.

### **Antibacterial assessment**

M-ZnO NPs were tested for their bactericidal activity against *S. aureus* and *E. coli* bacterial strains using an agar well diffusion assay. It is a relatively quick and effective test to determine antimicrobial activity. Different concentrations of M-ZnO NPs were pipetted into the well of agar plates. After that, the plates were incubated at 37 °C in the bacterial incubator for 24 hours. The bactericidal activity of MZnO NPs was in the form of a diameter of the Inhibition Zone (IZ). After 24 hours, the inhibition zones were observed.

### **Photocatalytic activity of ZnO Nps**

The prepared green ZnO NPs examined for the photocatalytic degradation of textile dyes. The photocatalytic activities of M-ZnO NPs was assessed for dye methylene blue and dye-containing textile wastewater. The degradation of dye was observed in three different conditions-1.) Dye degradation in direct sunlight with M-ZnO NPs, 2.) Dye degradation in sunlight without NPs, 3.) Dye degradation in dark (without sunlight) with M-ZnO Nps.

After certain time intervals, degradation of pollutants was observed and absorbance of dye pollutants at their respective wavelength was used to measure the residual dye amount measured using a UV-vis spectrophotometer

## **RESULT AND DISCUSSION**

### **Characterization of ZnO nanoparticles UV visible studies**

UV-vis absorption spectra are used to evaluate the optical properties of nanoparticles. UV-vis absorption spectra of green ZnO NPs shown in Figure 1 UV-vis absorption spectra reveal the mono dispersion of zinc oxide nanoparticles. The wavelength of absorption peaks of ZnO nanoparticles at 376 nm can be allied with ZnO intrinsic band-gap absorption. This happened because of the bounce of e<sup>-</sup> from the valence to the conduction band [10].

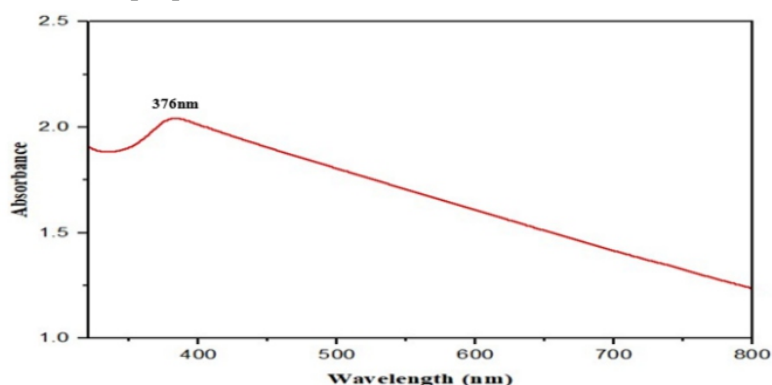


**Figure 1: Uv-vis absorption spectra of M-ZnO Nps**

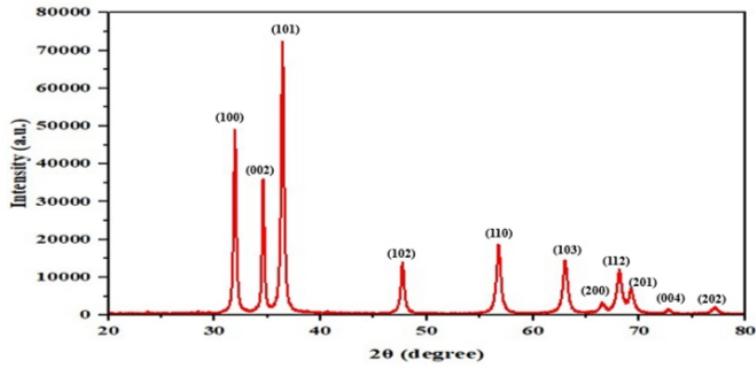


**Figure 2: XRD pattern of M-ZnO nanoparticles**

### XRD analysis

X-ray diffraction is used to determine the phase and crystallographic structure of a material. The green synthesized ZnO nanoparticles were characterized using powder XRD to confirm the nanoparticles as zinc and to examine the structural information and crystalline behaviour. The XRD profile of the optimized green ZnO NPs is reported in Figure 2. The prominent XRD peaks were obtained at  $2\theta$  values of  $31.79^\circ$ ,  $34.43^\circ$ ,  $36.28^\circ$ ,  $47.53^\circ$ ,  $56.5^\circ$ ,  $62.79^\circ$ ,  $67.83^\circ$ , and  $68.67^\circ$  Bragg peaks corresponding entirely to (100), (002), (101), (102), (110), (103), (112) and (201) indicating crystalline wurtzite structure of ZnO NPs and this data matched with JCPDS No. 36- 1451 [11, 12]

### SEM analysis

SEM images are used to predict the structural morphology of particles. SEM image of ZnO NPs (Figure 3) observed that the shape of most of the particles is spherical and the average size is between 70-120 nm. The SEM analysis of ZnO NPs coupled with the EDX spectrum confirms the zinc oxide particles and the presence of other elements.

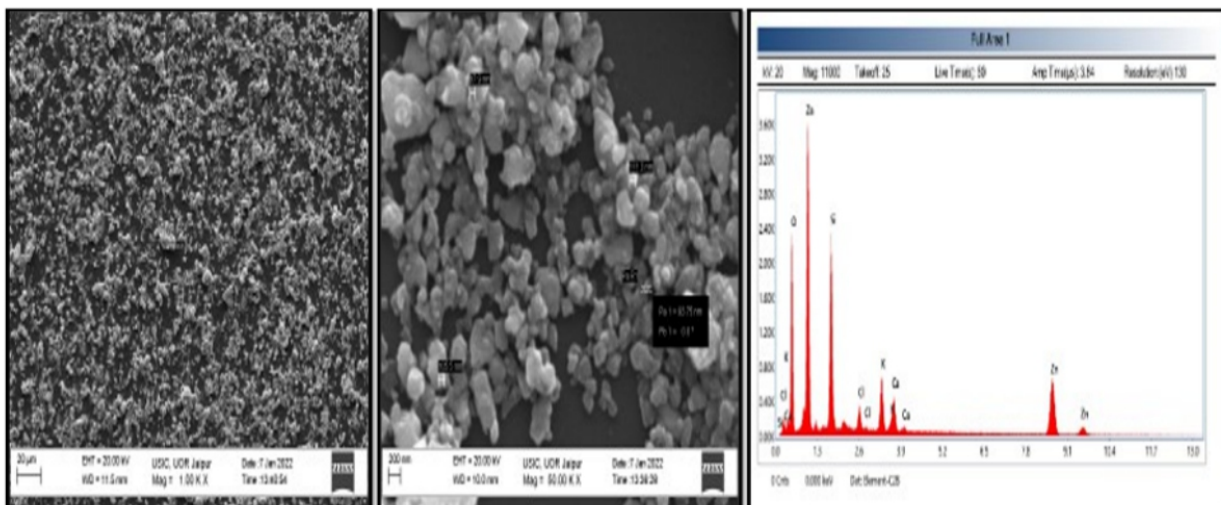


**Figure 3: SEM image of M-ZnO nanoparticles at different magnifications**

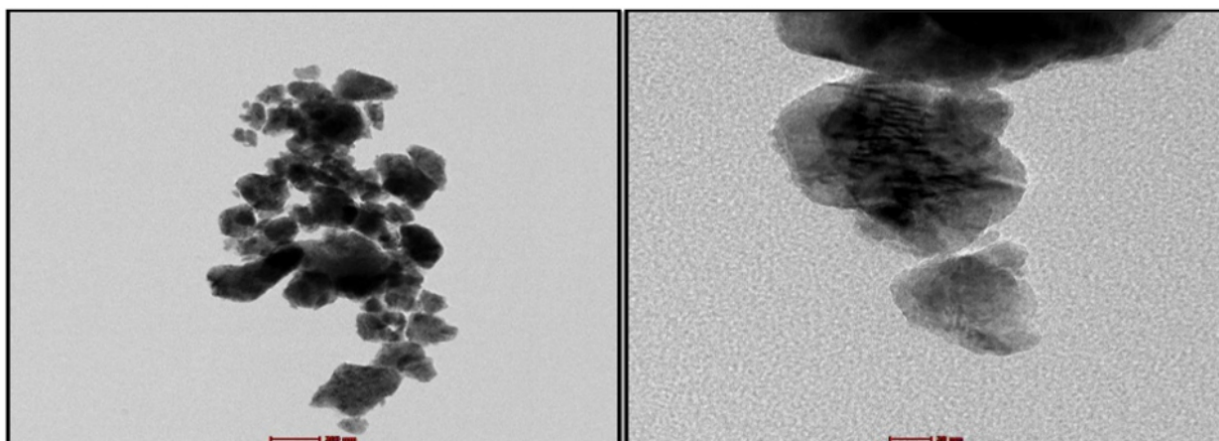


Figure 4: HR-TEM micrograph of M-ZnO NPs at different magnifications

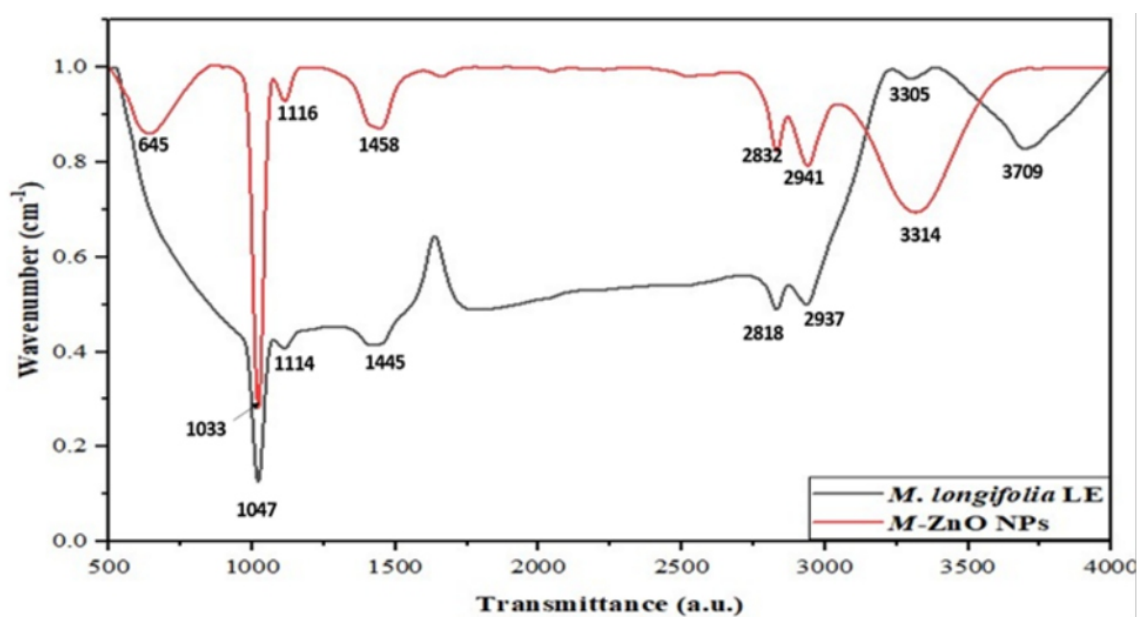


Figure 5: FTIR spectra of *M. longifolia* leaf extract and M-ZnO Nps

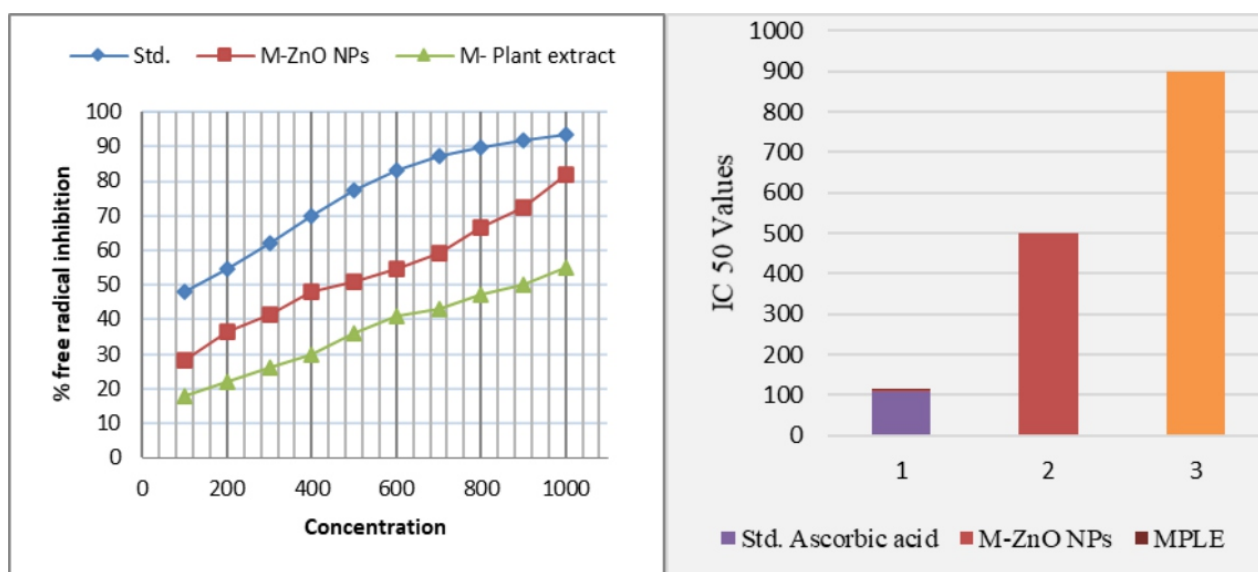
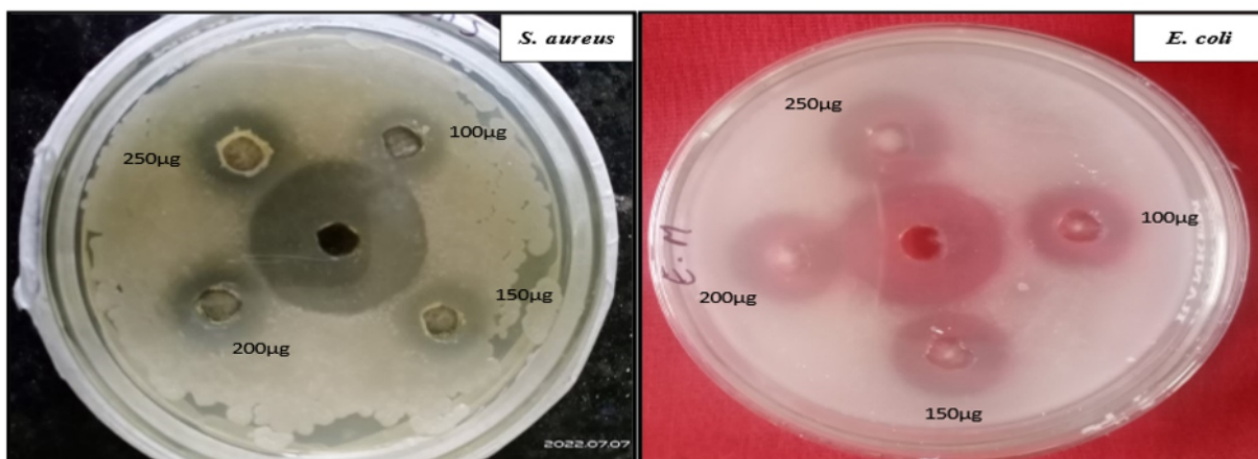


Figure 6: Free radicals inhibition percentage of *M. longifolia* leaf extract and M-ZnONPs and



**Figure 7: Inhibition zone of M-ZnO NPs against *S. aureus* and *E. coli* bacteria at different concentrations**

**Table 1: Antibacterial activity of *M. longifolia* leaf extract mediated synthesized ZnO nanoparticles**

| Bacteria                | Inhibition Zone (mm) |          |          |          |          |
|-------------------------|----------------------|----------|----------|----------|----------|
|                         | Standard             | 100µg/ml | 150µg/ml | 200µg/ml | 250µg/ml |
| <i>S. aureus</i>        | 32                   | 16       | 17       | 19       | 19       |
| <i>Escherichia coli</i> | 31                   | 19       | 20       | 22       | 23       |

The elemental inspection by the EDX spectrum shows that zinc is the major element that is present in the highest amount. Oxygen is also observed in the EDX spectrum which is related to the formation of ZnO NPs. Other elements observed in the EDX profile, are correlated with plant extracts that were used for ZnO NPs synthesis. Silica impurities were observed due to the glass slide used for thin film formation.

### TEM analysis

High resolution of the TEM was used to analyze the shape, size, and density of nanoparticles. The TEM image at different magnifications (20 and 200 nm) are shown in Figure 4. ZnO are quite monodisperse and nearly spherical in shape. However, some larger aggregates were also observed in the sample image because the aggregation is the result of the high surface energy of ZnO nanoparticles.

### FTIR analysis

The functional groups found in plant extracts that were utilised in the production of ZnO NPs were confirmed by FTIR spectroscopic analysis. For bio-reduced ZnO NPs, phytochemicals function as capping agents. The bio-reduction of ZnO NPs is carried



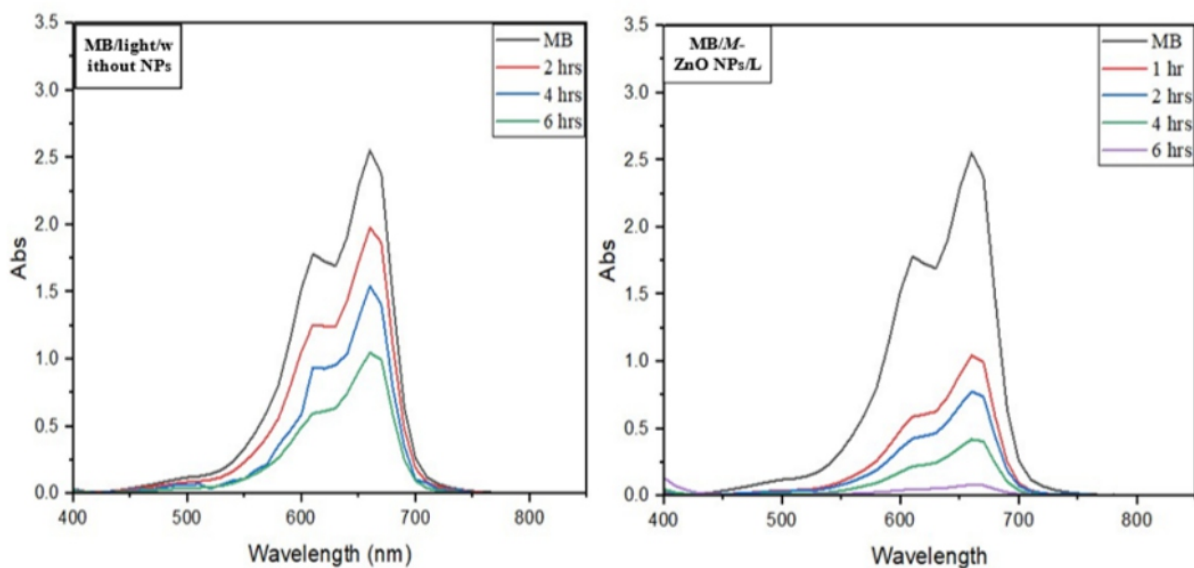


**Figure 8: MB dye degradation in the absence and presence of M-ZnO NPs under sunlight illumination**

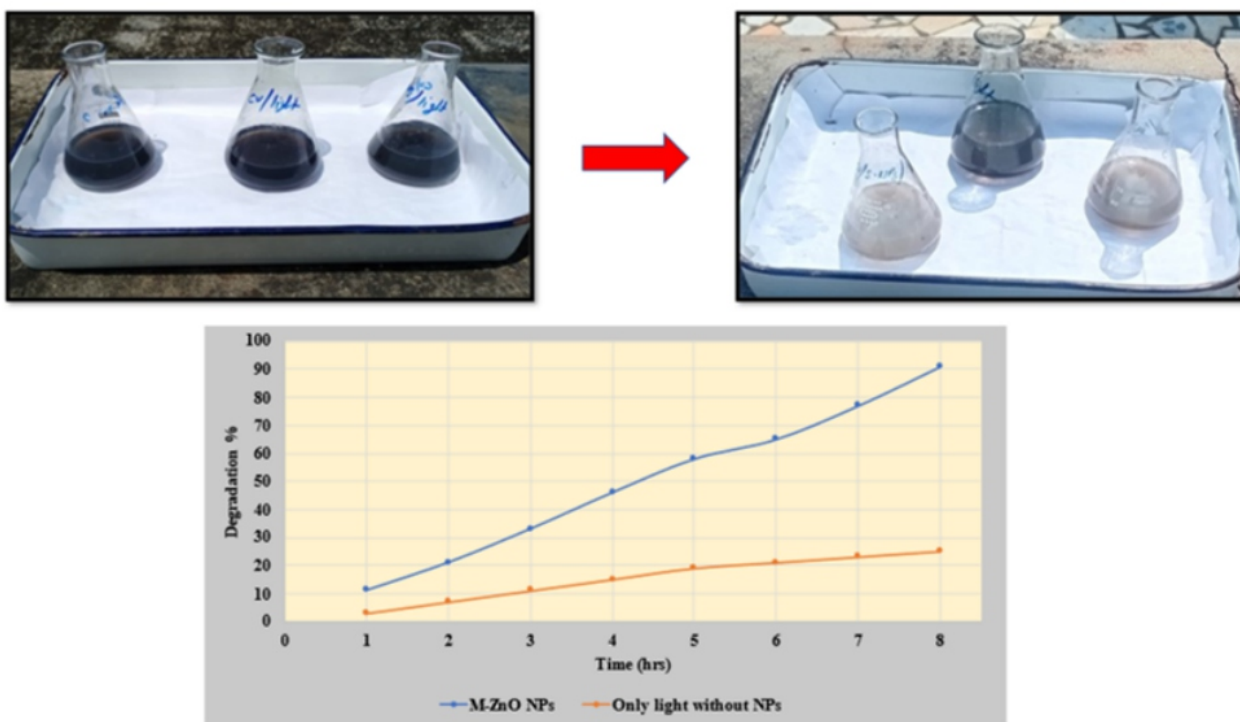


**Figure 9: Dye degradation percentage of textile wastewater in the presence and absence of ZnO Nps**

out using predetermined wave numbers to identify specific bond vibration peaks in the FTIR method. Figure 5 displays the FT-IR spectra of *M. longifolia* leaf extract and M-ZnO NPs. Because ZnO NPs span between 400 and 800  $\text{cm}^{-1}$ , the band at 645 is a sign of their presence. The absorption bands at 1047, 1114, 1445, 2818, 2937, 3305, and 3709  $\text{cm}^{-1}$  in *M. longifolia* leaf extract would be shifted to 645, 1033, 1116, 1458, 2832, 2941, 3314  $\text{cm}^{-1}$  in synthesized ZnO NPs. The absorption between 3200-3400 (peak band at 3314, 3305) indicates the O-H stretch of the phenol group [13]. The peak at 2818,

---

---

2937 for *M. longifolia* leaf extract and 2832, 2941 for M-ZnO NPs is because of C-H stretching vibrations in the aromatic compound. Further, the peak at 1033 and 1047 indicate the stretching between C-O of polyphenol. The absorption region at 942–1714  $\text{cm}^{-1}$  is due to C=N, C=O, NH, and C=C stretching vibrations of aromatic compounds [14].

### **Antioxidant activity of green ZnO nanoparticles**

The antioxidant potential of green synthesized ZnO NPs was evaluated against DPPH radical. DPPH (2,2-diphenyl-1-picryl-hydrazyl-hydrate) provides an easy method of determining antioxidant activity. DPPH was used as the free radical source and ZnO NPs were used as a radical scavenger. In the presence of ZnO NPs, the deep violet colour of the DPPH solution gradually changed into pale yellow colour. With the increase of ZnO NPs concentration, absorbance at 517 nm gradually decreases. The decrease in absorbance gives evidence of the radical scavenging ability of ZnO NPs.

DPPH solution was prepared by dissolving 0.004 gm DPPH in 100 mL of 80% methanol. In the presence of a free radical scavenger (ZnO NPs) that can change in absorbance at 517 nm which was determined spectrophotometrically. 80% of methanol was prepared by dilution of methanol with distilled water. In brief, a series of with 10 various concentrations values from 100  $\mu\text{l/ml}$  to 1000  $\mu\text{l/ml}$  of ZnO NPs solution was added and mixed with 3 ml DPPH solution. ZnO NPs solution was made by dispersing 1 mg NPs in 10 ml distilled water. The mixture was left in dark for 30 minutes. The absorbance against a blank (80% methanol), and a control sample (DPPH+ methanol) without the addition of a test sample and a series of different concentrations of the test samples (ZnO NPs) was recorded at 517 nm. The absorbance difference between control and test samples is considered as actual absorbance.

$$\frac{\text{Antioxidant activity Index}}{\frac{IC_{50} \text{ of the standard Ascorbic acid } (\mu\text{l/ml})}{IC_{50} \text{ of Sample } (\mu\text{l/ml})}} =$$

The IC<sub>50</sub> value for *M. longifolia* leaf extract is 900  $\mu\text{l/ml}$  and green ZnO NPs are 500  $\mu\text{g/ml}$  (Figure 6). results indicate that the antioxidant activity of *M. longifolia* leaf extract-mediated ZnO NPs is much higher than *M. longifolia* leaf extract.

### **Bactericidal activity of green ZnO nanoparticles**

Green synthesized ZnO nanoparticles were tested for their bactericidal activity against *S. aureus* and *E. coli* bacteria by agar well diffusion assay. Inhibition zone values were determined for the M-ZnO NPs at different concentrations (100  $\mu\text{g/ml}$ , 150  $\mu\text{g/ml}$ , 200  $\mu\text{g/ml}$ , and 250  $\mu\text{g/ml}$ ). ZnO NPs showed an excellent inhibitory effect against both *S. aureus* and *E. coli* bacteria due to their surface activity. In Figure 7, the diameter (mm) of inhibition zones of ZnO NPs solution around each well is shown. The result shows that inhibition zone diameter increase with the increasing concentration of ZnO NPs. *M. longifolia* leaf extract-mediated synthesized ZnO NPs are found the highest bactericidal activity against *E.*

---

---

coli (23 mm) at 250 µg concentration (Table 1). But Pachaiappan et al., 2021 [15]; reported that green synthesized ZnO NPs using *Justicia adhatoda* leaves extract showed higher bactericidal activity against *S. aureus* bacteria than *E. coli*. The result indicates that the bactericidal activity of green ZnO Nps depends on the concentration of NPs. Asha et al.(2022) [16]; reported that the antimicrobial potential of zinc oxide nanoparticles depends upon the size, smaller size NPs has better bactericidal effect than a larger one.

### **Photodegradation of Textile dyes**

In the sunlight irradiation but absence of M-ZnO, little degradation of MB dye was observed. The effect of both ZnO NPs on the photocatalytic degradation of MB was investigated and shown in Uv vis spectroscopy graphs. However, no photocatalytic degradation of MB dye was observed in dark conditions. The absorbance of dye-polluted water decreases with the increasing illumination time of sunlight irradiation. It is clearly seen in Uv-visible spectroscopy data that the relative concentration of dye reduced with sunlight illumination time. In the photocatalytic degradation process, the photogeneration of electron-hole pairs is generally responsible for the elimination of dye pollutants [17]. The degradation percentage of MB dye in the presence of ZnO NPs was calculated using the equation [18].

$$\text{Degradation \%} = \left[ A_o - \frac{A_t}{A_o} \right] \times 100$$

where  $A_0$  is the absorbance value at the initial stage and the absorbance at time “t” is  $A_t$ . After 6 hours, 96.08% degradation of MB dye was observed in the presence of M-ZnO NPs (Figure 8). Only 48% degradation was observed in the absence of nanoparticles. Anbuvaran et al. 2015 [1]; also reported the efficient photocatalytic property of green ZnO Nps against MB dye in sunlight illumination.

As we can see in Figure 9, textile industry contaminated water becomes transparent in the presence of M-ZnO NPs after 8 hours of sunlight illumination. After treatment of M-ZnO Nps, 91% of dye degradation was observed while only 25% degradation was observed in the absence of nanoparticles.

ZnO NPs have been shown to exhibit inhibitory and antibacterial properties, antioxidant properties and photocatalytic activity. It was also proven in previous Findings that green synthesis of nanoparticles improves their properties and reduced their hazards [19–21].

### **CONCLUSION**

In this study, Zinc oxide nanoparticles were synthesized by a simple, cost-effective, and eco-friendly approach using *Madhuca longifolia* plant leaves extract. The phytochemicals of *M. longifolia* leaf extract effectively work as reducing agents in ZnO NPs synthesis. The biogenic ZnO NPs were found to have 376 nm absorption spectra with a hexagonal wurtzite structure. Powdered XRD results confirm the

---

---

the crystalline structure of NPs. SEM and TEM images validated the formation of nanoparticles with 90 nm of average size. FTIR result showed the presence and role of phytochemicals in the synthesis of ZnO NPs. Results revealed that ZnO NPs showed significant antioxidant and antimicrobial activity. ZnO nanoparticles effectively photodegrade methylene blue dye under sunlight illumination. The objective of this study is to investigate the properties of bio-synthesized ZnO NPs which can help to reduce the hazards of chemically synthesized nanoparticles and enhance the efficiency of ZnO NPs. This study successfully facile green synthesized multifunctional ZnO nanoparticles using plant parts.

### **Abbreviations**

ZnO- zinc oxide, NPs- nanoparticles, M-ZnO NPs Madhuca longifolia leaf extract mediated zinc oxide nanoparticles, XRD- X-ray Diffraction, SEM- Scanning Electron Microscope, EDX- Energy Dispersive X-ray spectroscopy, TEM- Transmission Electron Microscope, FTIR- Fourier Transform Infrared spectroscopy, Uv-vis spectroscopy- Uv-visible spectroscopy.

### **ACKNOWLEDGEMENT**

This research is supported by JOINT CSIR-UGC and RUSA 2.0 MHRD grants.

### **Authors Contributions**

Rajani: conceptualization, formal analysis, investigation, writing-original draft;

Rishi Kesh Meena: investigations, writing-review, and supervision;

Preeti Mishra: conceptualization, writing-review, and editing.

### **Declarations of Competing Interest**

The authors declare that they have no competing interests or personal relationships that could have appeared to influence the work reported in this paper.

### **REFERENCES**

[1] M Ramesh, M Anbuvaran, and G Viruthagiri. Green synthesis of ZnO nanoparticles using *Solanum nigrum* leaf extract and their antibacterial activity. *Spectrochimica Acta Part A: Molecular and Biomolecular Spectroscopy*, 136(Pt B):864–870, 2015.

[2] P C Nethravathi, G S Shruthi, D Suresh, H Nagabhushana, and S C Sharma. *Garcinia xanthochymus* mediated green synthesis of ZnO nanoparticles: photoluminescence, photocatalytic and antioxidant activity studies. *Ceramics International*, 41(7):8680–8687, 2015.

[3] A Muthuvel, M Jothibas, and C Manoharan. Effect of chemically synthesis compared to biosynthesized ZnO-NPs using *Solanum nigrum* leaf extract and their photocatalytic, antibacterial and

---

---

*in-vitro* antioxidant activity. *Journal of Environmental Chemical Engineering*, 8(2):103705–103705, 2020.

[4] P M Rajani, S Kumari, P Saini, and R K Meena. Role of nanotechnology in management of plant viral diseases. *Materials today: Proceedings*, 69(1):1–10, 2022.

[5] H Sadiq, F Sher, S Sehar, E C Lima, S Zhang, H M Iqbal, and M Nuhanović. Green synthesis of ZnO nanoparticles from *Syzygium Cumini* leaves extract with robust photocatalysis applications. *Journal of Molecular Liquids*, 335, 2021. Article ID 116567.

[6] F Davar, A Majedi, and A Mirzaei. Green synthesis of ZnO nanoparticles and its application in the degradation of some dyes. *Journal of the American Ceramic Society*, 98(6):1739–1746, 2015.

[7] S Vasantharaj, S Sathiyavimal, P Senthil Kumar, V N Kalpana, G Rajalakshmi, M Alsehli, and A Pugazhendhi. Enhanced photocatalytic degradation of water pollutants using bio-green synthesis of zinc oxide nanoparticles (ZnO Nps). *Journal of Environmental Chemical Engineering*, 9(4), 2021. Article ID 105772.

[8] P Yadav, D Singh, A Mallik, and S Nayak. *Madhuca longifolia* (Sapotaceae), a review of its traditional uses, phytochemistry and pharmacology. *International Journal of Biomedical Research*, 3(7):291–305, 2012.

[9] J Sinha, V Singh, J Singh, and A K Rai. Phytochemistry, ethnomedical uses and future prospects of *Mahua* (*Madhuca longifolia*) as a food: a review. *J. Nutr. Food Sci*, 7(1), 2017. Article ID 1000573.

[10] D Suresh, P C Nethravathi, H Rajanaika, H Nagabhushana, and S C Sharma. Green synthesis of multifunctional zinc oxide (ZnO) nanoparticles using *Cassia fistula* plant extract and their photodegradative, antioxidant and antibacterial activities. *Materials Science in Semiconductor Processing*, 31:446–454, 2015.

[11] F T Thema, E Manikandan, M S Dhlamini, and M J M L Maaza. Green synthesis of ZnO nanoparticles via *Agathosma betulina* natural extract. *Materials Letters*, 161:124–127, 2015.

[12] M Zare, K Namratha, K Byrappa, D M Surendra, S Yallappa, and B Hungund. Surfactant assisted solvothermal synthesis of ZnO nanoparticles and study of their antimicrobial and antioxidant properties. *Journal of materials science & technology*, 34(6):1035–1043, 2018.

[13] K J Rao and S Paria. Green synthesis of silver nanoparticles from aqueous *Aegle marmelos* leaf extract. *Materials Research Bulletin*, 48(2):628–634, 2013.

[14] N Matinise, X G Fuku, K Kaviyarasu, N Mayedwa, and M Maaza. ZnO nanoparticles via *Moringa oleifera* green synthesis: Physical properties & mechanism of formation. *Applied Surface Science*, 406:339–347, 2017.

[15] R Pachaiappan, S Rajendran, G Ramalingam, N Dai-Viet Vo, P Mohana Priya, and M Soto Moscoso. Green synthesis of zinc oxide nanoparticles by *Justicia adhatoda* leaves and their

---

---

antimicrobial activity. *Chemical Engineering & Technology*, 44(3):551–558, 2021.

[16] S Asha, T C Bessy, J J Sherin, C V Kumar, M R Bindhu, S Sureshkumar, and A A Hatamleh. Efficient photocatalytic degradation of industrial contaminants by *Piper longum* mediated ZnO nanoparticles. *Environmental Research*, 208, 2022. Article ID 112686.

[17] I Kazeminezhad and A Sadollahkhani. Photocatalytic degradation of Eriochrome black-T dye using ZnO nanoparticles. *Materials Letters*, 120:267–270, 2014.

[18] C H Kwon, H Shin, J H Kim, W S Choi, and K H Yoon. Degradation of methylene blue via photocatalysis of titanium dioxide. *Materials Chemistry and Physics*, 86(1):78–82, 2004.

[19] H Agarwal, S V Kumar, and S Rajeshkumar. A review on green synthesis of zinc oxide nanoparticles- An eco-friendly approach. *Resource-Efficient Technologies*, 3(4):406–413, 2017.

[20] Y Y Chan, Y L Pang, S Lim, and W C Chong. Facile green synthesis of ZnO nanoparticles using natural-based materials: Properties, mechanism, surface modification and application. *Journal of Environmental Chemical Engineering*, 9(4), 2021. Article ID 105417.

[21] V N Kalpana and V Devi Rajeswari. A review on green synthesis, biomedical applications, and toxicity studies of ZnO NPs. *Bioinorganic chemistry and applications*, 2018. Article ID 3569758.

# Instructions for Authors

## Essentials for Publishing in this Journal

- 1 Submitted articles should not have been previously published or be currently under consideration for publication elsewhere.
- 2 Conference papers may only be submitted if the paper has been completely re-written (taken to mean more than 50%) and the author has cleared any necessary permission with the copyright owner if it has been previously copyrighted.
- 3 All our articles are refereed through a double-blind process.
- 4 All authors must declare they have read and agreed to the content of the submitted article and must sign a declaration correspond to the originality of the article.

## Submission Process

All articles for this journal must be submitted using our online submissions system. <http://enrichedpub.com/> . Please use the Submit Your Article link in the Author Service area.

---

## Manuscript Guidelines

The instructions to authors about the article preparation for publication in the Manuscripts are submitted online, through the e-Ur (Electronic editing) system, developed by **Enriched Publications Pvt. Ltd.** The article should contain the abstract with keywords, introduction, body, conclusion, references and the summary in English language (without heading and subheading enumeration). The article length should not exceed 16 pages of A4 paper format.

### Title

The title should be informative. It is in both Journal's and author's best interest to use terms suitable. For indexing and word search. If there are no such terms in the title, the author is strongly advised to add a subtitle. The title should be given in English as well. The titles precede the abstract and the summary in an appropriate language.

### Letterhead Title

The letterhead title is given at a top of each page for easier identification of article copies in an Electronic form in particular. It contains the author's surname and first name initial .article title, journal title and collation (year, volume, and issue, first and last page). The journal and article titles can be given in a shortened form.

### Author's Name

Full name(s) of author(s) should be used. It is advisable to give the middle initial. Names are given in their original form.

### Contact Details

The postal address or the e-mail address of the author (usually of the first one if there are more Authors) is given in the footnote at the bottom of the first page.

### Type of Articles

Classification of articles is a duty of the editorial staff and is of special importance. Referees and the members of the editorial staff, or section editors, can propose a category, but the editor-in-chief has the sole responsibility for their classification. Journal articles are classified as follows:

#### Scientific articles:

1. Original scientific paper (giving the previously unpublished results of the author's own research based on management methods).
2. Survey paper (giving an original, detailed and critical view of a research problem or an area to which the author has made a contribution visible through his self-citation);
3. Short or preliminary communication (original management paper of full format but of a smaller extent or of a preliminary character);
4. Scientific critique or forum (discussion on a particular scientific topic, based exclusively on management argumentation) and commentaries. Exceptionally, in particular areas, a scientific paper in the Journal can be in a form of a monograph or a critical edition of scientific data (historical, archival, lexicographic, bibliographic, data survey, etc.) which were unknown or hardly accessible for scientific research.

### **Professional articles:**

1. Professional paper (contribution offering experience useful for improvement of professional practice but not necessarily based on scientific methods);
2. Informative contribution (editorial, commentary, etc.);
3. Review (of a book, software, case study, scientific event, etc.)

### **Language**

The article should be in English. The grammar and style of the article should be of good quality. The systematized text should be without abbreviations (except standard ones). All measurements must be in SI units. The sequence of formulae is denoted in Arabic numerals in parentheses on the right-hand side.

### **Abstract and Summary**

An abstract is a concise informative presentation of the article content for fast and accurate Evaluation of its relevance. It is both in the Editorial Office's and the author's best interest for an abstract to contain terms often used for indexing and article search. The abstract describes the purpose of the study and the methods, outlines the findings and state the conclusions. A 100- to 250-Word abstract should be placed between the title and the keywords with the body text to follow. Besides an abstract are advised to have a summary in English, at the end of the article, after the Reference list. The summary should be structured and long up to 1/10 of the article length (it is more extensive than the abstract).

### **Keywords**

Keywords are terms or phrases showing adequately the article content for indexing and search purposes. They should be allocated heaving in mind widely accepted international sources (index, dictionary or thesaurus), such as the Web of Science keyword list for science in general. The higher their usage frequency is the better. Up to 10 keywords immediately follow the abstract and the summary, in respective languages.

### **Acknowledgements**

The name and the number of the project or programmed within which the article was realized is given in a separate note at the bottom of the first page together with the name of the institution which financially supported the project or programmed.

### **Tables and Illustrations**

All the captions should be in the original language as well as in English, together with the texts in illustrations if possible. Tables are typed in the same style as the text and are denoted by numerals at the top. Photographs and drawings, placed appropriately in the text, should be clear, precise and suitable for reproduction. Drawings should be created in Word or Corel.

### **Citation in the Text**

Citation in the text must be uniform. When citing references in the text, use the reference number set in square brackets from the Reference list at the end of the article.

### **Footnotes**

Footnotes are given at the bottom of the page with the text they refer to. They can contain less relevant details, additional explanations or used sources (e.g. scientific material, manuals). They cannot replace the cited literature.

The article should be accompanied with a cover letter with the information about the author(s): surname, middle initial, first name, and citizen personal number, rank, title, e-mail address, and affiliation address, home address including municipality, phone number in the office and at home (or a mobile phone number). The cover letter should state the type of the article and tell which illustrations are original and which are not.

### **Address of the Editorial Office:**

**Enriched Publications Pvt. Ltd.**  
S-9, IInd FLOOR, MLU POCKET,  
MANISH ABHINAV PLAZA-II, ABOVE FEDERAL BANK,  
PLOT NO-5, SECTOR -5, DWARKA, NEW DELHI, INDIA-110075,  
PHONE: - + (91)-(11)-45525005



